



Wind turbine test Vestas V27-225 kW

Markkilde Petersen, Søren

Publication date:
1990

Document Version
Publisher's PDF, also known as Version of record

[Link back to DTU Orbit](#)

Citation (APA):
Markkilde Petersen, S. (1990). *Wind turbine test Vestas V27-225 kW*. Risø-M No. 2861

General rights

Copyright and moral rights for the publications made accessible in the public portal are retained by the authors and/or other copyright owners and it is a condition of accessing publications that users recognise and abide by the legal requirements associated with these rights.

- Users may download and print one copy of any publication from the public portal for the purpose of private study or research.
- You may not further distribute the material or use it for any profit-making activity or commercial gain
- You may freely distribute the URL identifying the publication in the public portal

If you believe that this document breaches copyright please contact us providing details, and we will remove access to the work immediately and investigate your claim.

RISO-M--2861

DE91 763376

RISØ-M-2861

WIND TURBINE TEST VESTAS V27-225 kW

*Søren Markkilde Petersen
The Test Station For Wind Turbines
Department for Meteorology and Wind Energy
Risø*

Abstract. The report describes fundamental measurements performed on a Vestas-V27-225 kW pitch regulated wind turbine. The measurements carried out and reported here comprises the power output, system efficiency, energy production, transmission efficiency, rotor power, rotor efficiency, air-brakes efficiency, structural dynamics, loads at cut-in and braking, yaw error statistics, flapwise root bending moment and rotor thrust.

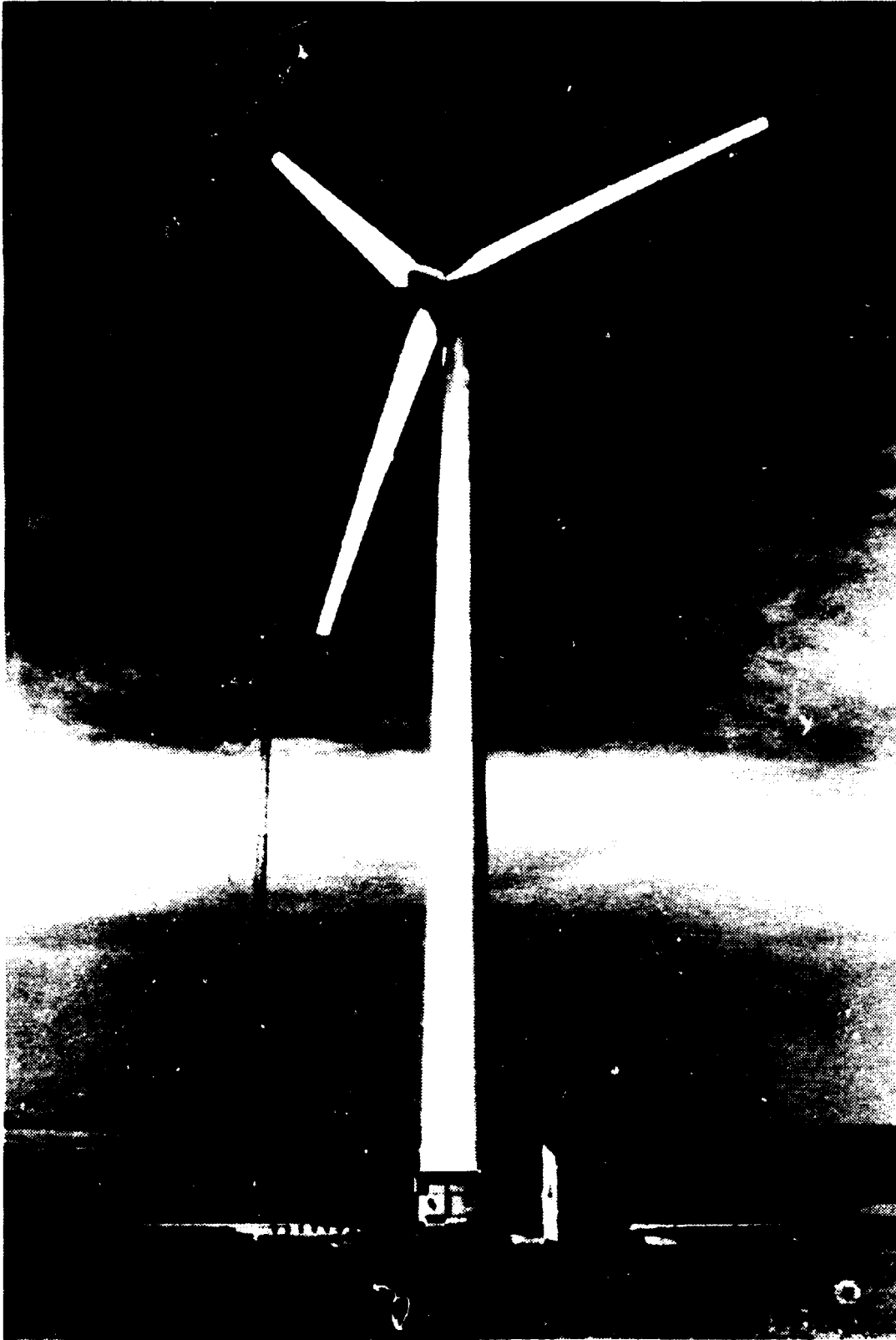
October 1990

Risø National Laboratory, DK-4000 Roskilde, Denmark

The wind turbine was tested according to a contract with:
Vestas Wind System A/S, Smed Hansensvej 27, 6990 Lem.

ISBN 87-550-1684-7
ISSN 0418-6435

Grafisk Service Center, Rissø 1990.



The picture shows the Vestas V27 erected at the Test Station on stand 4.

CONTENTS

	Page
1. INTRODUCTION	7
2. THE WIND TURBINE	7
2.1 Technical description	7
2.2 Control system and operation	11
2.3 Instrumentation	11
3. THE TEST STATION	16
3.1 The Test Site	16
3.2 Data acquisition and analysis	20
3.3 The load for the turbine	20
4. SAFETY TESTS	21
4.1 Test of mechanical brake	21
4.2 Test of air brakes	27
5. POWER PERFORMANCE MEASUREMENTS	28
5.1 Power curve measurements	28
5.2 Annual energy production	30
6. STRUCTURAL MEASUREMENTS	31
6.1 Eigenfrequencies of the fundamental modal shapes	31
6.2 Structural response during operation	38
6.3 Structural measurements summary	42
7. MEASUREMENTS OF ELECTRICAL CHARACTERISTICS	43
7.1 Measurements of current at cut-in	43
7.2 Electric power quality	48
8. OTHER DESIGN RELATED MEASUREMENTS	53
8.1 Transmission efficiency	53
8.2 Rotor performance	55
8.3 Yaw error measurements	57
8.4 Flapwise root bending moment	60
8.5 Axial rotor thrust	62
SUMMARY	63
REFERENCES	65

1. INTRODUCTION

The Vestas V27 wind turbine was erected at The Test Station in March 1989 on stand 4. The basic tests were completed in December 1989. The measurements made correspond to the basic measurement program, which is developed and carried out at the Test Station for Windmills at Risø. This program is described in Refs. 1 and 4.

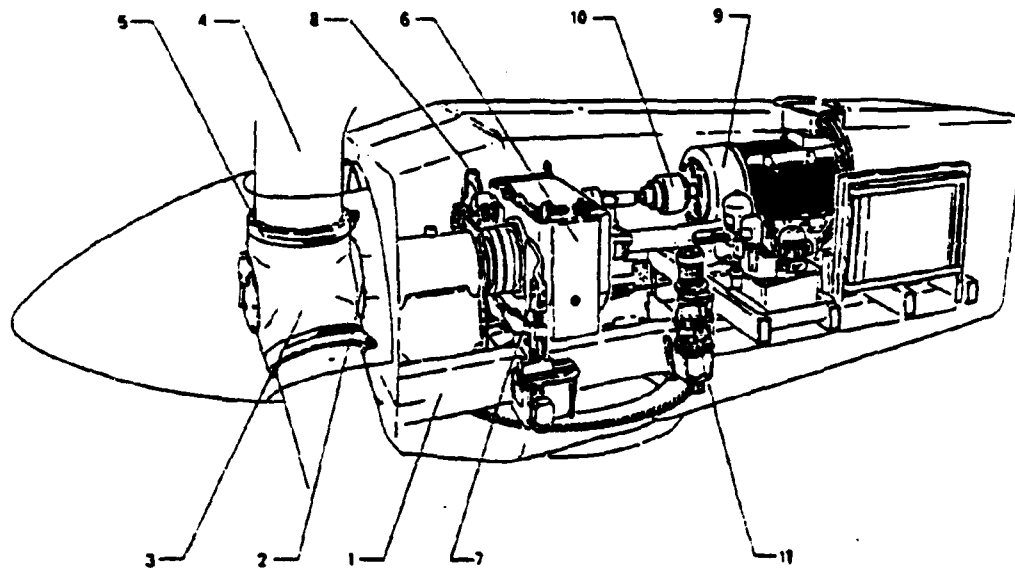
2. THE WIND TURBINE

In this chapter the wind turbine is described to the extent necessary to understand the measurements carried out. The rotor is surveyed in detail as this is the most important part of the turbine. The principles of the control system are outlined as they are the basis for understanding the safety system and operation of the turbine. Finally, the installation of the sensors on the turbine are sketched. This might aid in interpreting the test results.

2.1 Technical description.

The layout of the nacelle is shown in Fig. 2.1.1. The wind turbine has a three-bladed upwind rotor with pitch regulated cantilevered GRP blades on a cast iron hub. The rotor shaft is held by two main bearings. The disc brake is mounted on the fast running shaft. The gearbox is mounted behind the shaft on the nacelle frame. The double wound generator is connected to the gearbox by a stiff clutch.

Yawing of the nacelle is carried out by an electrical motor controlled by a wind vane, mounted on top of the nacelle. The electrical control system is mounted in the nacelle and in the bottom of the tower. The tower is a tube tower in one section. Further specifications are listed in Table 2.1.2.



- 1. Main frame
- 2. Main shaft
- 3. Hub
- 4. Blade
- 5. Blade bearings
- 6. Gear box
- 7. Gear lever arm
- 8. Disc brake
- 9. Generator
- 10. Coupling
- 11. Yaw motor

Fig. 2.1.1. Principal lay out of the nacelle.

*Table 2.1.2. Technical description of Vestas V 27.***Rotor**

Power regulation:	Pitch
Number of blades:	3
Rotor diameter (measured):	27.0 m
Swept area:	573 m²
Hub height:	31.5 m
Rotor speed (low rpm):	33.0 rpm
Rotor speed (high rpm):	43.0 rpm
Tilt:	4.0 deg
Coning:	0 deg
Blade tip angles (meas.):	-0.7 deg
:	-0.7 deg
:	-0.2 deg
Tip angle during operation:	-1 to 30 deg
Direction of rotation	
(looking downwind):	clockwise

HUB

Hub construction:	cast iron
--------------------------	------------------

BLADES

Make:	Vestas Wind System A/S
Type:	cantilevered GRP
Spar material:	GRP
Shell material:	GRP
Blade length:	13.0 m
Profiled blade length:	11.5 m
Root chord:	1.29 m
Tip chord:	0.47 m
Blade twist:	13 deg
Blade profiles:	NACA 63-200 series
	(14-35%) Trailing edge modified.
Air brake:	Pitch controlled

GEARBOX

Make:	Hansen
Type:	helical two stage
Gear ratio:	1:23.4

GENERATOR

Make:	Siemens
Type:	asynchronous
Nominal power:	225/50 kW
Synchronous speed:	1000/750 rpm

MECHANICAL BRAKE

Type:	disc brake
No. of calibers:	2
Position:	high speed shaft
Activation:	electrohydraulic

CONTROL SYSTEM

Make:	Vestas Wind systems A/S
Cut-in system:	thyristor
Logic system:	microprocessor
Yaw system:	wind vane and yaw motor

TOWER

Type:	tubular in one section
Height:	31 m

WEIGHTS

Blade:	600 kg
Rotor incl. hub and blades:	2900 kg
Nacelle without rotor:	7900 kg
Tower:	12000 kg
Total weight (approx.):	22800 kg

2.2. Control system and operation.

The control system is made by Vestas Wind System A/S. It has a full automatic operation mode, where a lot of parameters are supervised. For a detailed description of the parameters we refer to Ref. 3.

It has not been the aim of the wind turbine test to examine the control system itself but some tests directly involve the control system. These are the test of the mechanical brake, the measurement of current at cut-in and measurement of the power curve. For the last mentioned, the strategy for the control system is of major importance. The automatic operation is carried out in the following way.

At wind speeds below cut-in, the blades are pitched in order to increase the driving torque. At low wind conditions the turbine with pitch angle about 45 deg acts like an anemometer.

When the wind has reached a certain level sufficient for the turbine to produce electrical power, the pitch angle is regulated as a function of the rotational speed. When synchronous speed condition is met the pitch regulation causes the acceleration of the rotor to stop. The rotational speed is kept approximately constant for a small period of time, establishing stable electrical conditions. The small generator is connected to the grid when a subsequently random passage of synchronous speed occurs. The connection of the main generator to the electrical grid is by similar means. In the following this procedure is called a normal connection.

When a generator shift is initiated due to changes in the wind speed the power output is regulated to 0 kW and the generator is disconnected. The rotor is then accelerated or decelerated to either high or low synchronous rotational speed, and a normal connection procedure takes place.

At wind speed above cut-out wind speed (25 m/s) the power is regulated to 0 kW. The generator is disconnected and the pitch angle is regulated to about 80 deg.

2.3. Instrumentation

The overall instrumentation for the basic measurements and structural measurement which are not reported here is shown in Fig. 2.3.1. The sensors used for the instrumentation are listed in Table 2.3.2.

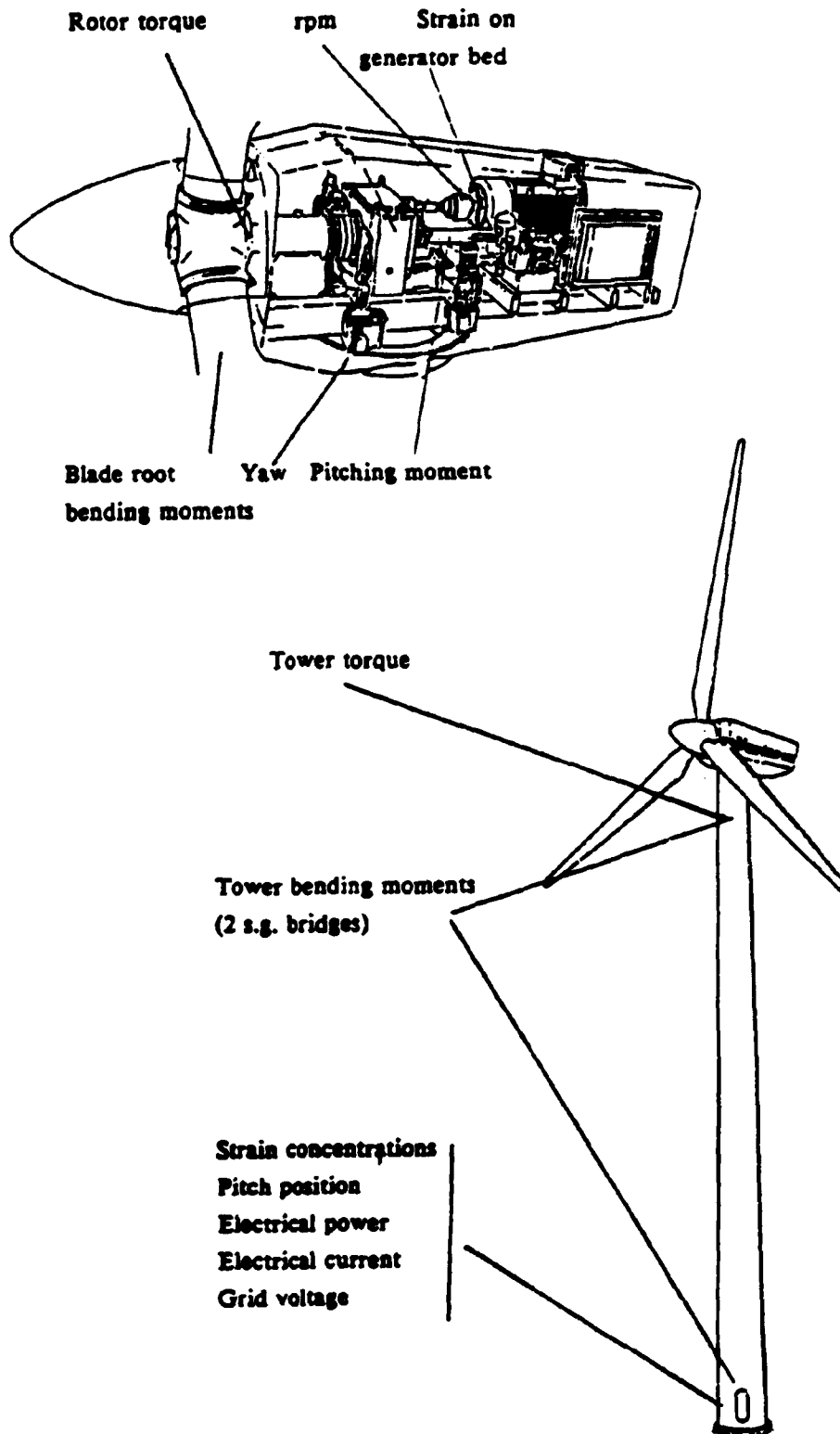


Fig. 2.3.1. Instrumentation of Vestas V27

Table 2.3.2.

Parameter	Sensor/transmitter	Range	Calibration
Wind speed	Rise cup-anemometer, model 83, With three cups and two pulses per revolution. Used with Rise f/v transmitter P1225.	approx 0 to 36 m/s -5V to +5V	approx 3.6 V/18 m/s
Wind direction	Rise resolver wind vane model 80. Used with a Rise transmitter P1182.	0° - 360° 0 V - 3,6 V	100°/V
Air temperature	Pt 500 thermometer, Din 43760. Used with Rise P1182 transmit- ter	-25°C to +35°C -5V to +5V	6°C/V+5°C
Barometric pressure	YSI, Model 214. Used with Rise P1261 transmitter	790 to 1091 mB -5V to +5V	30.10mB/V +940,67 mB
Electric power	DEIF measurement transformer on all three phases. Connected to DEIF Inwatt-GS Wattconverter	Typically -5/3. Pnom to 5/3. Pnom -5V to 5V	Typically 1/3. Pom/V
Electric current	LEM current sensor on one phase		
Grid voltage	Voltage sensor on one phase		
Rotor rota- tional	Inductive switch, mounted at a disc with holes on the fast running shaft	Typically 0 to 5/3. Nnom	Typically 1/3. Nnom/V

Parameter	Sensor/transmitter	Range	Calibration
Rotor torque	Torque strain gauge bridge, mounted on main shaft, connected to an FM one-channel telemetry equipment, Hottinger transmitter M12555A (Rise box P1141A) and Hottinger receiver/preamplifier EV2510A (Rise box P1142). Transmission through two coils wound around the shaft. Battery supply through Rise battery	box P1389.	On the site
Yaw	Rotary encoder, mounted with a tooth wheel on the yaw tooth ring. Signal converted by Borthel Electronics type 86120501	0° to 360° -5V to +5V	36°/V
Pitch position	The signal from the distance transducer, already mounted on the turbine is connected to the Rise equipment		
Blade root bending moments	Two bending moment strain gauge bridges, mounted on one blade root, connected to Johne & Reilhofer 8 channel telemetry system		On the site
Bending moments in tower	Bending moments in tower are measured in three sections, close to top, close to bottom and at the middle. At each section two strain gauge bridges are mounted in perpendicular directions (E-W, N-S). S.g.'s connected to four channel H B M s.g. amplifiers		On the site
Torsional moment in tower	Torsional moment is measured close to top with a full strain gauge bridge. S.g. connected to a four channel HMB s.g. amplifier		On the site

Parameter	Sensor/transmitter	Range	Calibration
Pitching moment	Is measured as a force on the pitch governor with a full s.g. bridge. S.g. connected to a four channel H B M s.g. amplifier		In Workshop
Strain on generator bed	One s.g. bridge connected to a four channel H B M s.g. amplifier		In Workshop
Strain concentrations at entrance door in tower	1/4 bridge s.g.'s mounted close to door weldings		

3. THE TEST STATION

The conditions for a wind turbine test are very important for the interpretation of the results of the measurements. In the following, the conditions for the Test Station are described in chapters comprising the topography and climatology data acquisition and analysis, and the electric load conditions for the turbine.

3.1. The test site.

The Test Station for Windmills is situated at Risø National Laboratory, 5 km north of Roskilde and 30 km west of Copenhagen. The test stands are positioned on a rather flat area close to Roskilde Fjord (see Fig. 3.1.1). From the fjord, which is about 200 m away, the ground is gently raised to an elevation of about 9 m in average at the stands. The prevailing winds are westerly coming from the fjord.

The meteorological conditions at the test site are measured continuously on a central meteorological tower.

The wind speed is measured at 3, 10, 20 and 33 m height, and for the period May 1982 to January 1986 the statistical wind distribution has been calculated.

For the four heights the Weibull parameters for the wind speed distributions are shown in Table 3.1.2. Generally the measured distributions fit very well to the Weibull distributions.

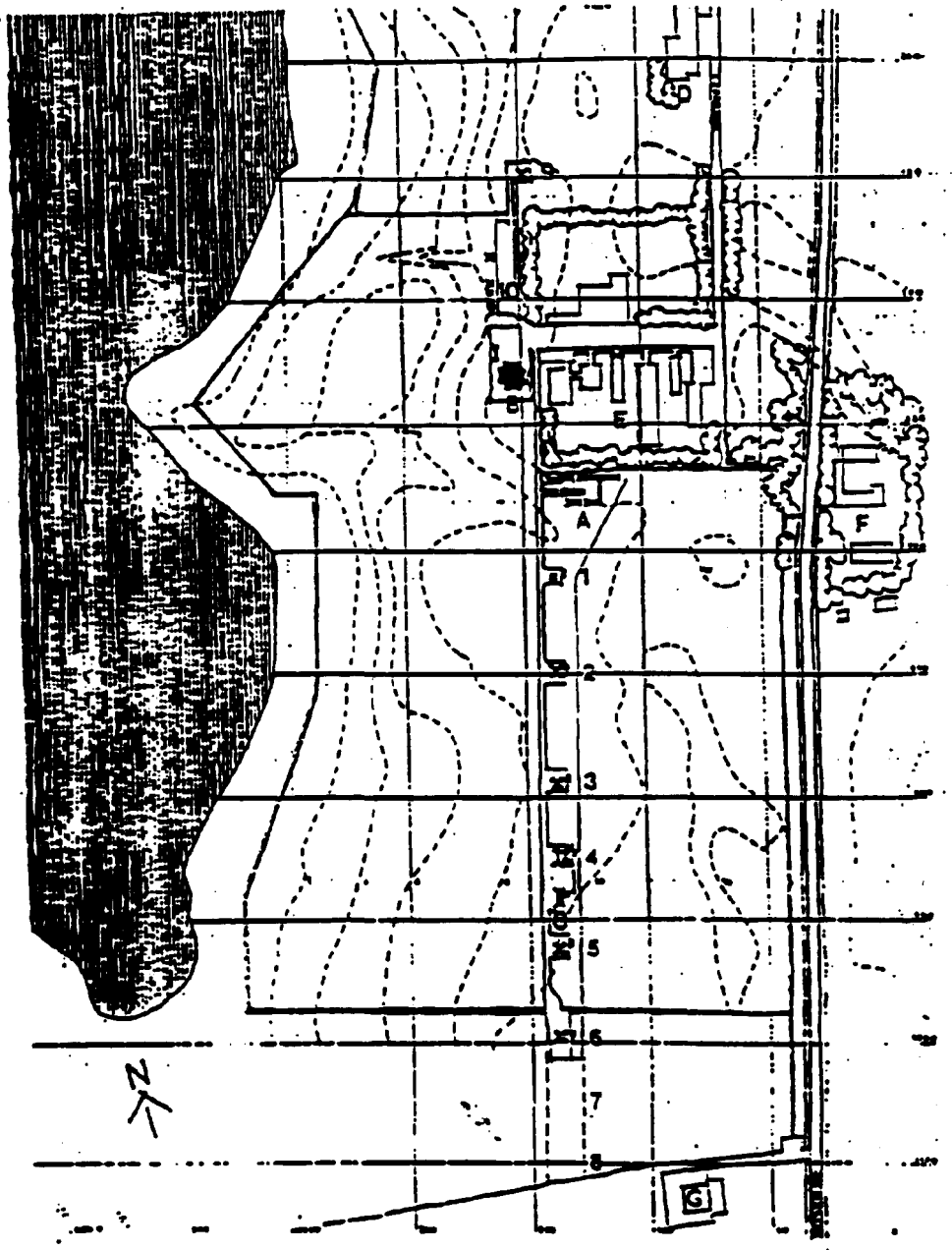


Fig. 3.1.1. Topology at the site.

<u>33 m</u>					<u>20 m</u>				
	A	C	f	V		A	C	f	V
	m/s		%	m/s		m/s		%	m/s
N	4.9	1.77	6.0	4.3	N	4.2	1.75	5.9	3.8
NE	4.1	2.04	5.0	3.6	NE	3.4	2.00	4.9	3.0
E	6.4	2.10	10.9	5.6	E	5.7	1.98	10.8	5.0
SE	7.1	2.41	17.0	6.3	SE	6.6	2.38	16.9	5.9
S	5.5	2.21	9.7	4.8	S	4.8	2.17	9.6	4.2
SV	6.2	2.34	18.2	5.5	SV	5.7	2.26	18.3	5.0
V	7.7	2.12	20.6	6.9	V	7.4	2.13	20.9	6.5
NV	6.5	1.68	12.6	5.8	NV	6.3	1.76	12.7	5.6
Total 6.5 2.00 100.0 5.7					Total 6.0 1.93 100.0 5.3				

<u>10 m</u>					<u>3 m</u>				
	A	C	f	V		A	C	f	V
	m/s		%	m/s		m/s		%	m/s
N	3.8	1.73	5.8	3.4	N	3.2	1.71	5.6	2.99
NE	2.9	1.86	4.8	2.6	NE	2.5	1.75	4.6	2.2
E	4.8	1.87	11.9	4.3	E	3.8	1.66	13.4	3.4
SE	5.8	2.25	16.4	5.1	SE	4.7	1.97	16.6	4.1
S	4.3	2.03	9.9	3.8	S	3.5	1.88	9.9	3.1
SV	5.4	2.21	18.8	4.7	SV	4.5	2.14	17.3	4.0
V	7.1	2.17	19.8	6.3	V	5.7	2.10	20.2	5.1
NV	5.9	1.77	12.5	5.3	NV	4.8	1.80	12.3	4.2
Total 5.5 1.87 100.0 4.8					Total 4.4 1.79 100.0 4.0				

Table 3.1.2. Weibull parameters for wind speed distributions at the test site.

The annual mean wind speed is 5.3 m/s at 20 m height and 5.7 m/s at 33 m. The prevailing wind directions are western, which also are the wind directions used for the most measurements on the wind turbines. Stationary masts for wind speed measurements are placed perpendicular to the row of test stands, which has an orientation from 15 deg north to 195 deg south. Figure 3.1.3 shows a sketch of the test stands.

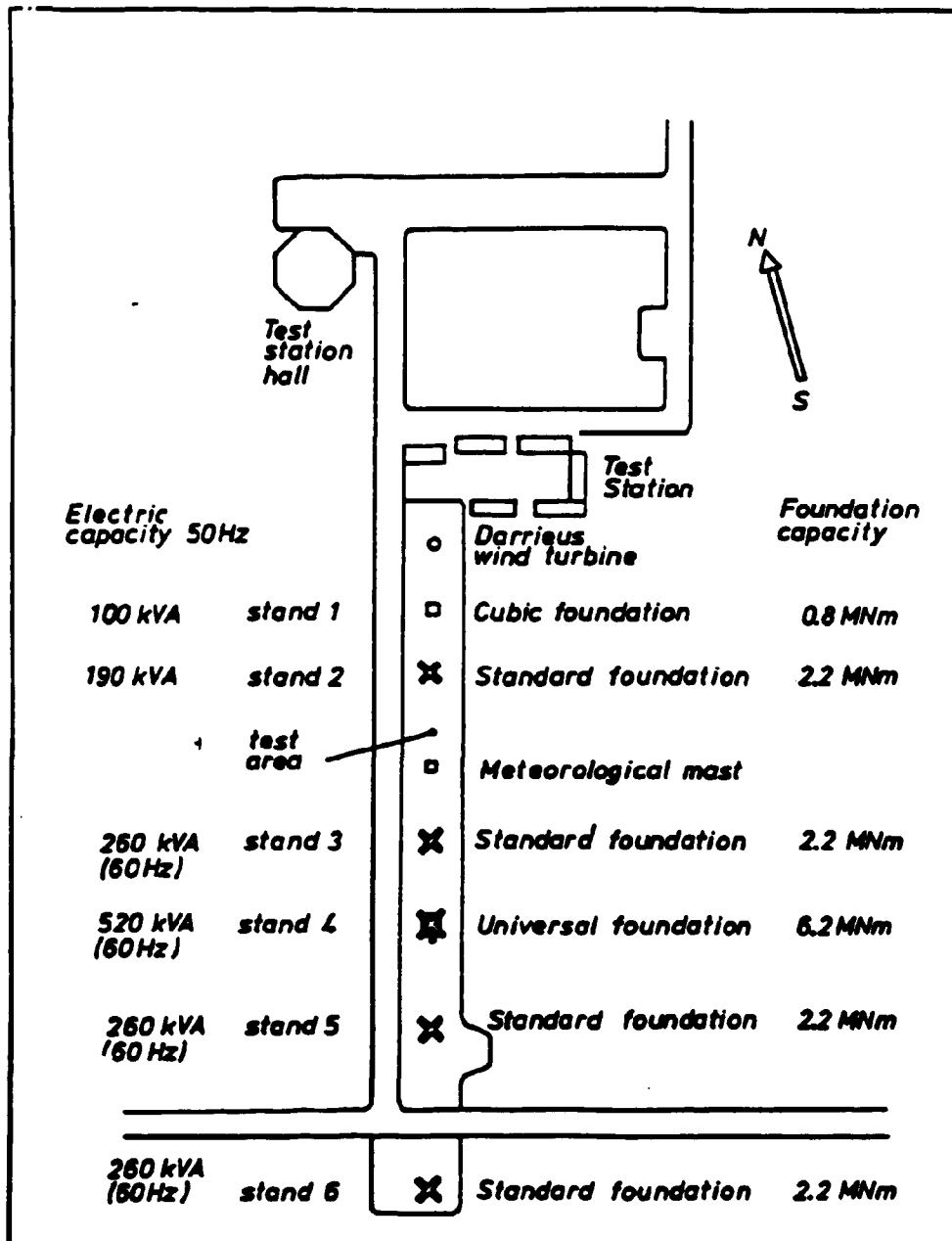


Fig. 3.1.3. The test stands for wind turbine testing.

3.2. Data acquisition and analysis.

The measurement system at the Test Station has multi-channel DC-cables from each test stand to the computer room for transferring data. The sensors are supplied with power at each test stand, and the signals are transferred with a voltage range from - 5V to + 5V.

At the computer room all channels pass through a filter that protects the computer equipment from lightning. Afterwards they pass through a low-pass filter module with a cut-off frequency of 0.4 Hz or 20 Hz. Alternatively the signal can pass directly through.

After the filter module the signals can go directly to a strip chart recorder for time-trace recording, to a spectrum analyzer for frequency analyzes or to the computer for data acquisition. The analog signals are converted to digital representation with a 12 bit resolution for the +5V voltage range.

For measurements of power curve, transmission efficiency and air brakes efficiency the 0.4 Hz filter and a sample frequency of 1 Hz is used.

The electric power is corrected to the standard air density of 1.225 kg/m³, corresponding to an air temperature of 15 °C and barometric pressure of 1013.3 mbar, accordance with ECN-217-recommendation (ref. 2).

The sampled data are block averaged with 30 seconds and 10 minutes. Data analysis is performed using the Method of Bins with a bin width of 0.5 m/s. The centers of the bins are at each half and full m/s. For each bin the wind speed, electric power, rotor rotational speed and rotor torque is averaged and for electric power and rotor torque the standard deviation is calculated.

For power curve measurements only a 90 sector from 240 deg at southwest to 330 deg at northwest is included in the data analysis. Only bins with more than 3 averages are included. The power curve is extended by 30-sec averages at higher wind speeds, but only for at least 3 averages.

For further details about the power performance procedure see ref. 2.

3.3. The load for the turbine.

The turbine was tested on a 50 Hz, 3 x 400 V grid, which was connected to a 1 MW transformer raising the voltage level to 10 kV.

4. SAFETY TESTS

A windmill has one or more safety systems with the purpose of keeping the turbine from overloading in emergency situations. Testing of these systems is therefore important to assure safe operation. In this chapter measurements concerning the mechanical brake and the air brake are reported.

4.1. Test of mechanical brake.

The mechanical brake was tested in two ways, performing successive shut-down sequences and recording loads in each case. Either the "PAUSE" or "EMERGENCY STOP" button are pressed, or the turbine was disconnected from the grid using the main switch. The braking sequences are performed at relatively low and high wind conditions. During recording of the time track signals, 20 Hz filter modules were used on all measured parameters.

Figure 4.1.1 shows the result of a push-button stopping procedure at a rotational speed of 43 rpm at about 7 m/s. The power was approximately 80 kW on the generator when the "PAUSE" button was activated.

The pitch regulation is activated and decreases the shaft power and electrical power simultaneously in a linear sense, in a time span of about 0.9 sec. After that period a cut-out of the generator is performed. At cut-out no increase in torque is noted.

Figure 4.1.2 shows the result of a push-button stopping procedure at a rotational speed of 43 rpm at high wind about 14 m/s. The power was approximately 210 kW on the generator when the "PAUSE" button was activated.

The pitch regulation is activated and decreases the shaft power and electrical power simultaneously, in a time span of about 2.3 sec.

After that period a cut-out of the generator is performed. As at low wind conditions no increase in torque is noted at cut-out.

Figure 4.1.3 and 4.1.4 shows the grid disconnection using the "EMERGENCY STOP" button at 7 m/s. The electrical power before the disconnection is about 90 kW. The delay time from cutting of the grid to full brake torque is about 0.9 sec.

The average brake torque is about 56 kNm, and the maximum torque is about 64 kNm. It corresponds to about 1.21 times the rotor torque at rated power.

When stopped, the rotor oscillates at a frequency of roughly 1.23 Hz and a max amplitude of 78 kNm. The damping of the system brings it to a full stop in roughly 7 cycles.

The braking sequence by switching off the main switch at a high wind speed at 16 m/s is shown in figure 4.1.2. When using the main switch the pitch position can't be measured because the signal is taken directly from the control system, which also is disconnected. The power is about 220 kW at cut-out. A small acceleration of the rotor is seen. The maximum rotational speed is about 46 rpm. Full brake torque is reached 0.9 seconds after cut-out of the generator. The mean brake torque is again about 54 kNm and the maximum torque is about 64 kNm. A drive train eigenfrequency of 5.2 Hz is seen during this phase.

When stopped, the rotor again oscillates at a frequency of roughly 1.23 Hz. The damping brings it to a full stop in roughly 4 cycles.

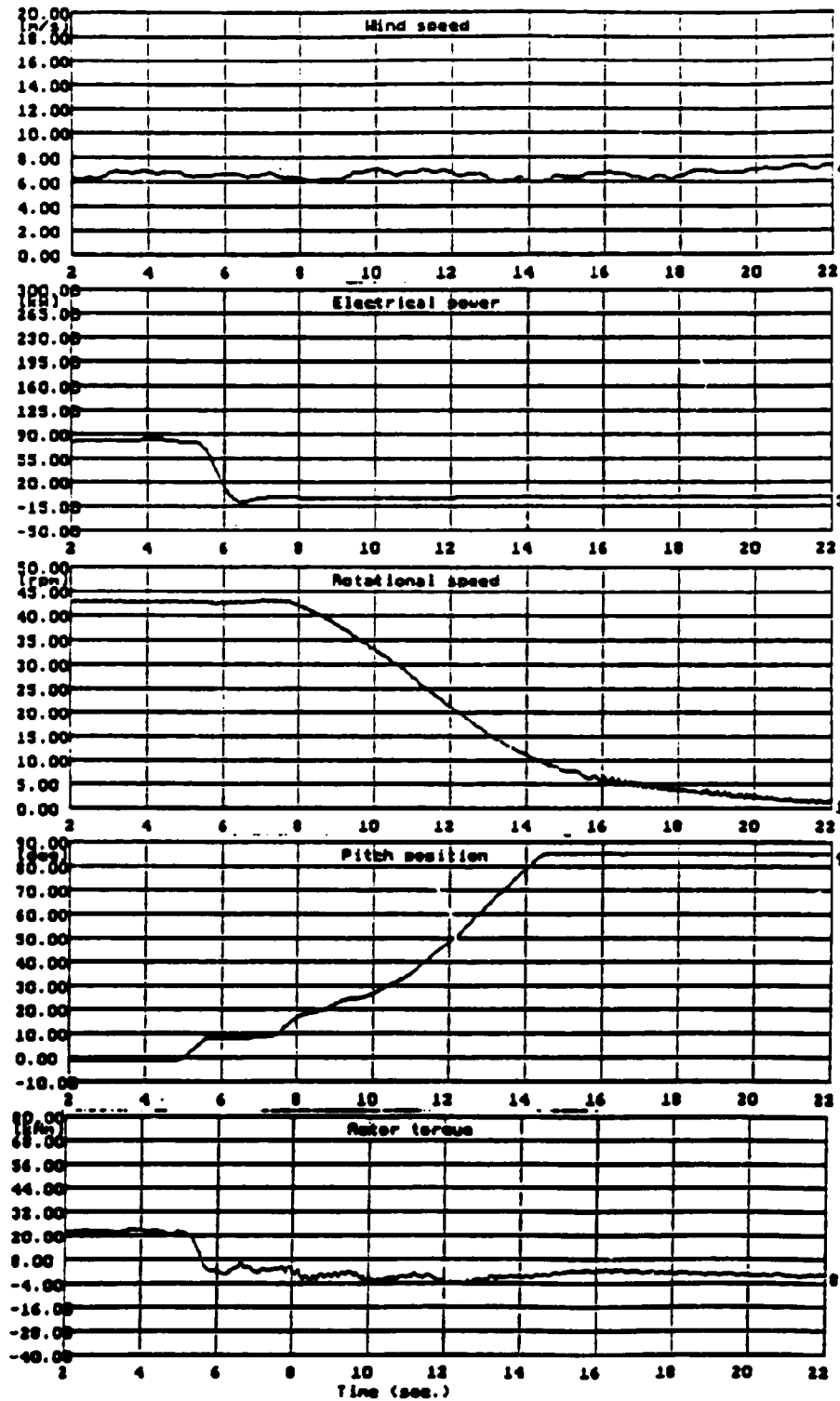


Fig. 4.1.1. Test of the Mechanical brake ("PAUSE" button).

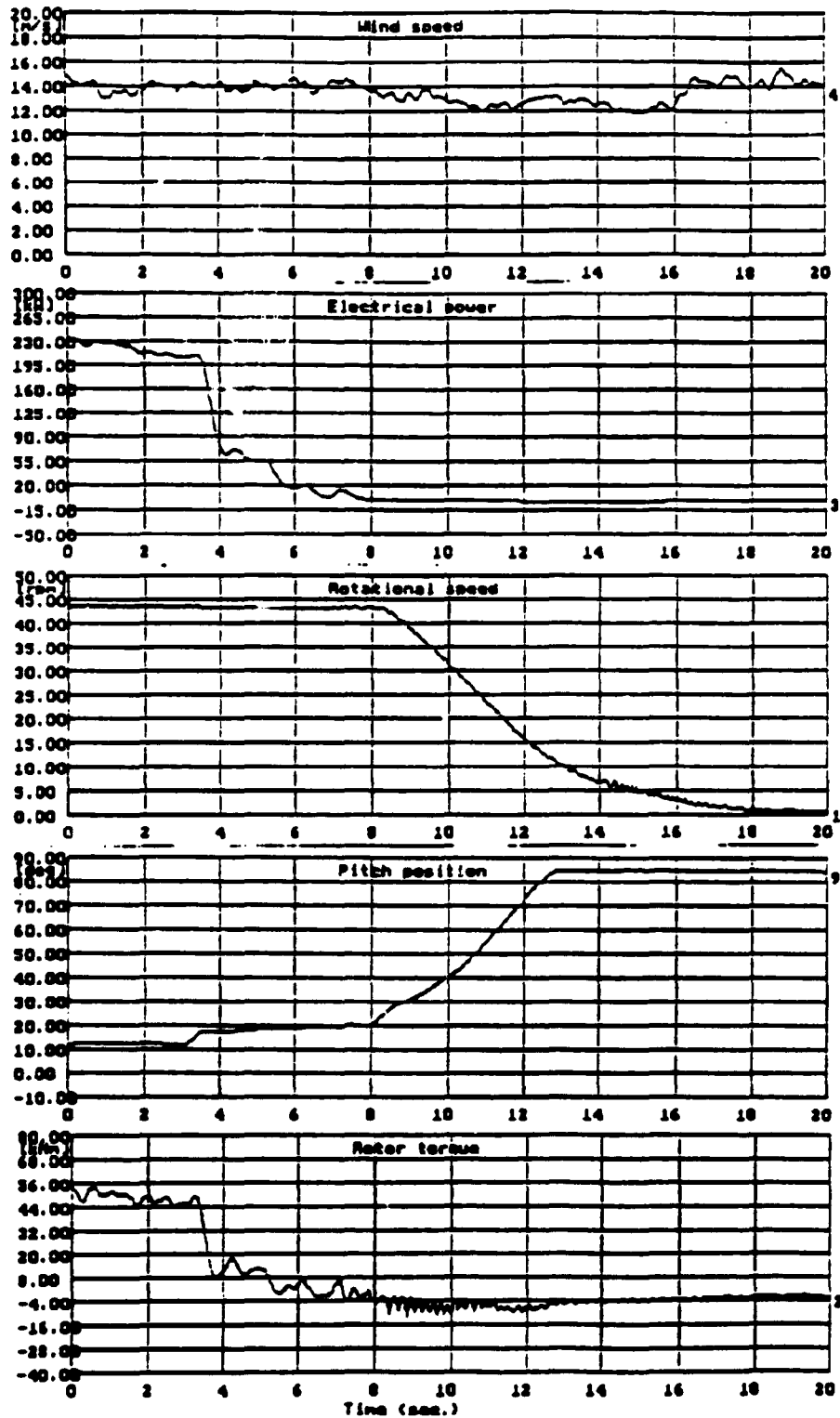


Fig. 4.1.2. Test of the Mechanical brake ("PAUSE" button).

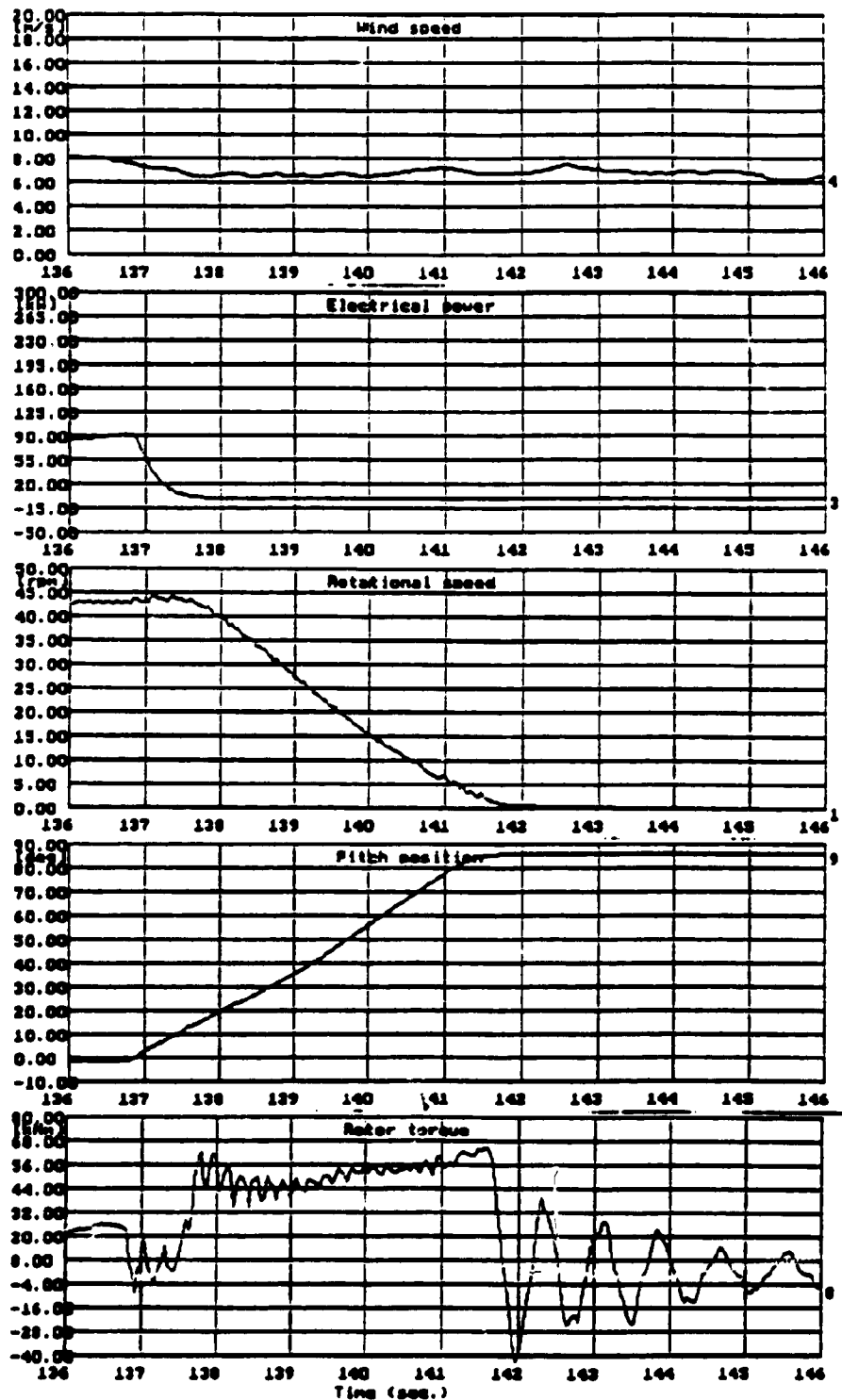


Fig. 4.1.3. Mechanical brake ("EMERGENCY STOP" button).

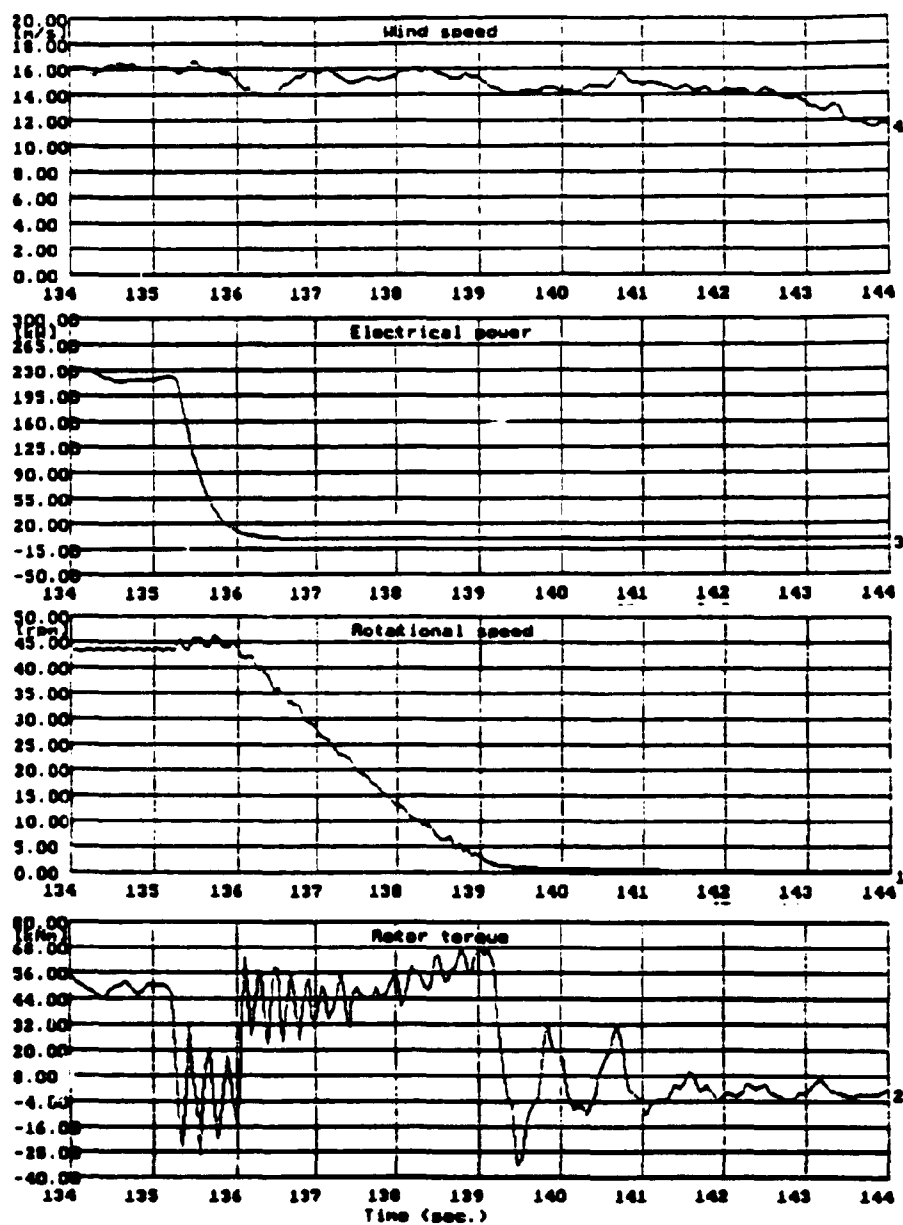


Fig. 4.1.4. Mechanical brake (Main switch).

4.2. Test of air brakes

In emergency situations the blades turn to a tip angle of approximately 88 degrees by stored hydraulic pressure.

When the turbine is idling at this tip angle the rotational speed is always kept below 2 rpm even at high wind speed above 25 m/s.

The yaw system is not active when the turbine is idling. The efficiency of the blade settings during idling is only tested when the rotor is upwind.

The efficiency of the blade settings, with the rotor in upwind position is quite well.

5. POWER PERFORMANCE MEASUREMENTS

The performance of the wind turbine is an important measurement because the economy is to a large extent based on the ability of the turbine to produce power.

The power curve measurement and analysis are in accordance with the ECN-217 July, 1989. Recommendations for an European Wind Turbine Standard on Performance Determination (Ref. 2).

5.1. Power Curve Measurements.

The power curve was measured in a period from 15.05.1989 to 03.08.1989. In the period 13 runs were carried out with wind from the westerly wind sector.

Below 70% of nominal power the data are corrected to a standard air density of 1.225 kg/m³ and averaged. Above 70% power no correction is performed. The actual air density during the measurements at high performance was differing less than 0.2 % from the standard air density. The power curve and the turbine efficiency are shown and tabulated in Fig. 5.1.1. Fig.5.1.1 is identically with Measurement summary No. 6.1, September 1989.

Measurement summary

No. 6.1, September 1989

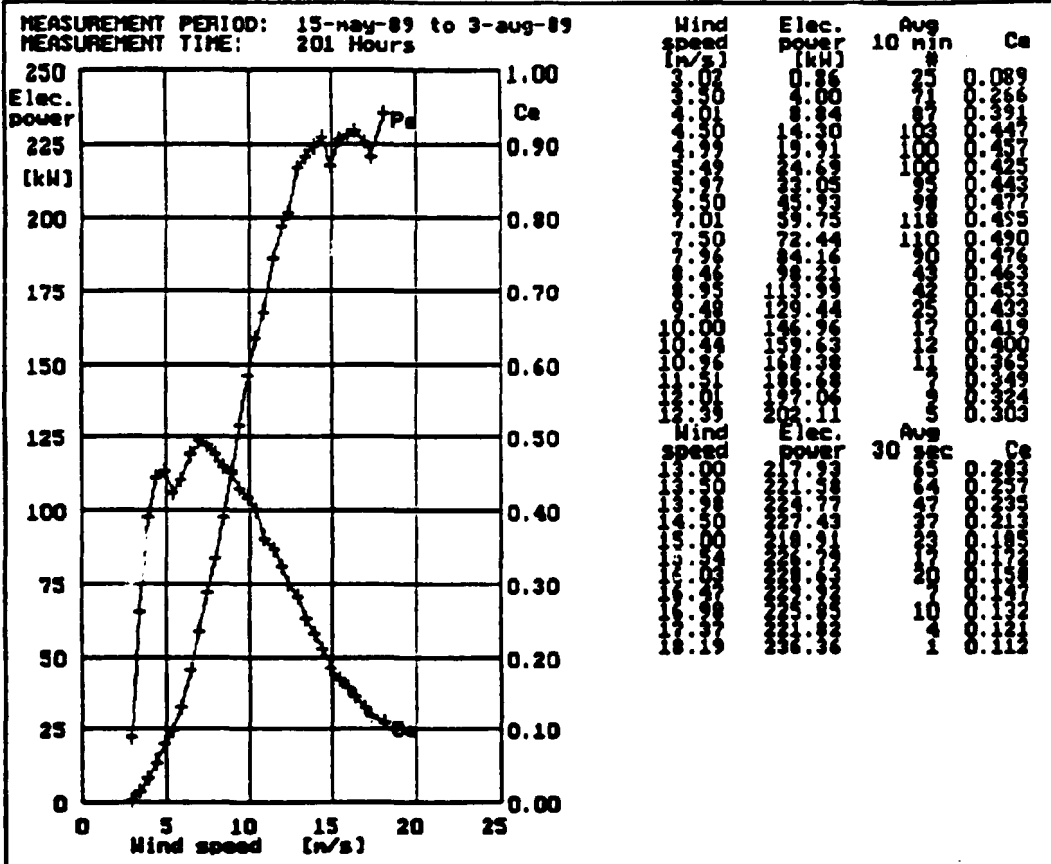
POWER CURVE MEASUREMENT

WIND TURBINE: Vestas U27-225kW

Measurement setup: anemometer at
hub height 50 m from wind turbine
in upwind position. Wind direction
+45 deg. from anemometer mast.

Analysis in accordance with:
ECN-217 July, 1989. Recommendations
for an European Wind Turbine Stan-
dard on Performance Determination.

POWER CURVE



ANNUAL ENERGY PRODUCTION

Weibull distribution (100 % availability) (Hub height = 31.5 m)		Form factor = 1.50 1.75 2.00 2.25 2.50					
Roughness class	Annual production [MWh]	Wind speed [m/s]	[MWh]	[MWh]	[MWh]	[MWh]	[MWh]
0	779.6	4.0	107.7	107.7	107.7	107.7	107.7
1	584.2	10.0	107.7	107.7	107.7	107.7	107.7
2	470.4	11.0	107.7	107.7	107.7	107.7	107.7
3	304.2	11.0	107.7	107.7	107.7	107.7	107.7

Fig. 5.1.1. Power Performance.

The wind turbine starts production at 3.0 m/s and at 7.0 m/s it reaches the maximum efficiency of 49.5% at 59.75 kW. Nominal power is reached at 15.5 m/s. The maximum measured power is 236 kW at 18.19 m/s. The pitch regulation limits the power output to about 225 kW. The stop wind speed condition at 25 m/s was not reached.

5.2. Annual Energy production

Annual energy production is calculated for a 100% availability and with the power curve data from Chapter 5.1. The power output between max wind speed and the stop wind speed is considered the same as at the highest measured wind speed.

Calculation of the annual energy production is based on Weibull distributions, which for a form factor of two equals the Reyleigh distribution (see Ref. 1). The calculation is divided into two different categories. One deals with world-wide application, where the annual mean wind speed is related to the hub height and five different form factors. For other form factors the annual energy production can be interpolated between the data given in Fig. 5.1.1.

For Danish application the Danish Wind Atlas method is used (see Ref. 5). The annual energy production is calculated for the four clean roughness classes 0, 1, 2 and 3 at hub height. The data is presented in Fig 5.1.1. For the actual 31.5 m hub height of the tested wind turbine, the annual energy production at roughness class 0 is calculated as 780 MWh and correspondingly for class 1, 2 and 3 to 584, 470 and 304 MWh.

6. STRUCTURAL MEASUREMENTS

Structural measurements deal with measurements of vibrations in the construction. Their purpose is to determine the shapes of the structural vibrational modes and the corresponding eigenfrequencies.

The analysis is based on measurements of the edgewise and flapwise blade root bending moment on one blade, the rotor shaft torque, the tower bending moment and the tower torsion (refer to paragraph 2.3 for description of strain gauge locations).

6.1. Eigenfrequencies of the fundamental modal shapes.

By stopping the rotor the only force exciting the structure will be the wind. Due to the broad and flat frequency spectrum of the wind, the structure will mainly vibrate in its structural vibrational modes. That facilitates the identification of the modal shapes. The measurements are performed with the rotor in three different positions as indicated in the figures. The instrumented blade is either horizontal, pointing vertically upward or downward. The pitch angle during the measurements is -1° which is the pitch setting during normal operation.

The five important modes (the five lowest eigenfrequencies) that can be observed in the frequency spectra, Fig. 6.1.6, has been identified on the basis of the survey of modal shapes of a wind turbine presented in Ref. 6. The shape and eigenfrequency of the five modes are described below.

Vibrational mode 1.

Mode 1 is dominated by the first tower bending mode. In the first tower bending mode the tower moves roughly as a massless cantilevered beam with a fixed mass at the end. The tower mode is coupled with the first symmetric rotor mode, in which the nacelle is rigidly fixed, and the three blades oscillates in phase in the first flapwise blade mode, Fig. 6.1.1.

The eigenfrequency is lowered slightly by the in-phase coupling with the first symmetric rotor mode. From Fig. 6.1.6 and Fig. 6.1.8. the eigenfrequency can be seen to be 0.84 Hz.

Vibrational mode 2.

This mode is dominated by the first asymmetric rotor mode but couples in phase with the first tower torsional mode, Fig. 6.1.2. The blade movement will be minimum in the vertical positions and maximum in the horizontal positions. From Fig. 6.1.6 and Fig. 6.1.9 the eigenfrequency can be seen to be 1.96 Hz.

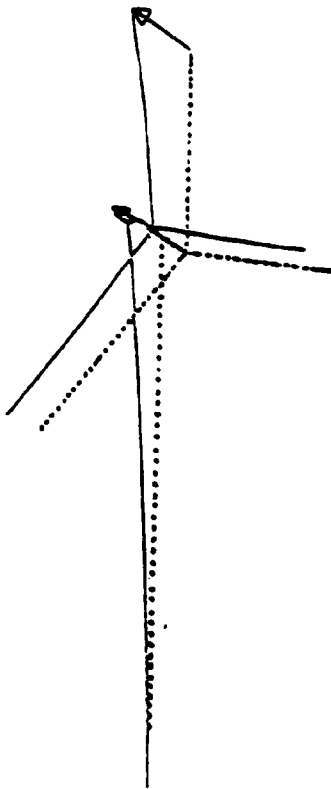


Fig. 6.1.1 Vibrational mode 1.
Eigenfrequency 0.84 Hz.

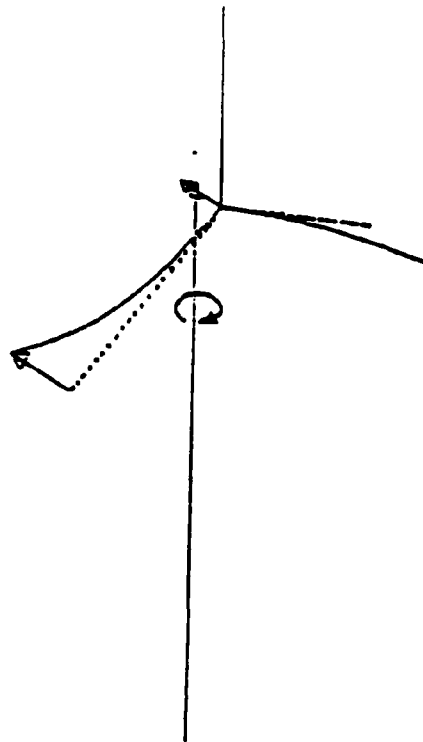


Fig. 6.1.2 Vibrational mode 2.
Eigenfrequency 1.96 Hz.

Vibrational mode 3.

The mode is dominated by the first asymmetric rotor mode, but coupled in-phase with the second tower bending mode. The blade movement will be at a minimum in the horizontal positions and at a maximum in the vertical positions, see Fig. 6.1.3. From Fig. 6.1.6 and Fig. 6.1.10 the eigenfrequency can be seen to be 2.00 Hz. The frequency is almost equal to the frequency to mode 2, because the stiffness vertical and horizontal are almost identical.

Vibrational mode 4.

The mode is dominated by the first symmetric rotor mode. In the first symmetric rotor mode the nacelle is rigidly fixed, and the three blades oscillates in phase in the first flapwise blade bending mode. Fig. 6.1.4.

The eigenfrequency is slightly increased due to counterphase coupling with the first tower bending mode. From Fig. 6.1.6 the eigenfrequency can be seen to be 2.36 Hz.

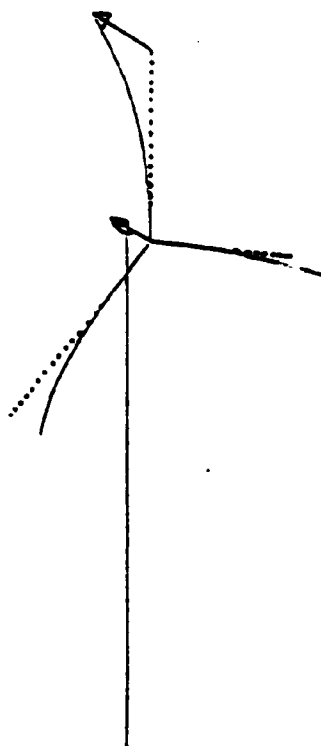


Fig. 6.1.3 Vibrational mode 3.
Eigenfrequency 2.00 Hz.

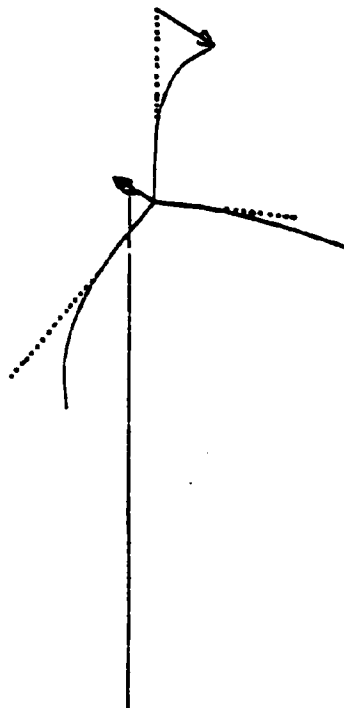


Fig. 6.1.4 Vibrational mode 4.
Eigenfrequency 2.36 Hz.

Vibrational mode 5.

The mode is dominated by the first torsional tower mode but counter phase coupled with the asymmetric rotor mode, Fig. 6.1.5. In the first torsional tower mode the tower vibrates roughly as a massless shaft fixed at one end and having a rotating inertia at the other end. From Fig. 6.1.9 the eigenfrequency can be seen to be 5.04 Hz.

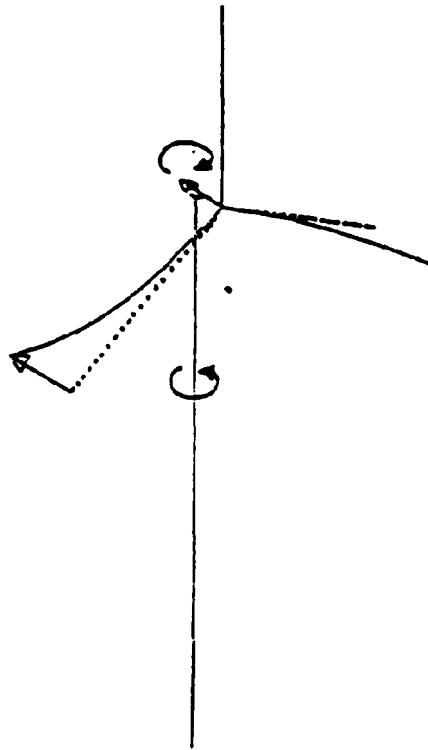


Fig. 6.1.5 Vibrational mode 5. Eigenfrequency 5.04 Hz.

Other modes.

Within the frequency interval of the described modes, however, there is one more mode with an eigenfrequency of 1.40 as can be seen on Fig. 6.1.7. It is the first shaft torsion mode with the mechanical disc brake activated coupled in-phase with the first edgewise blade mode. During operation this mode does not exist.

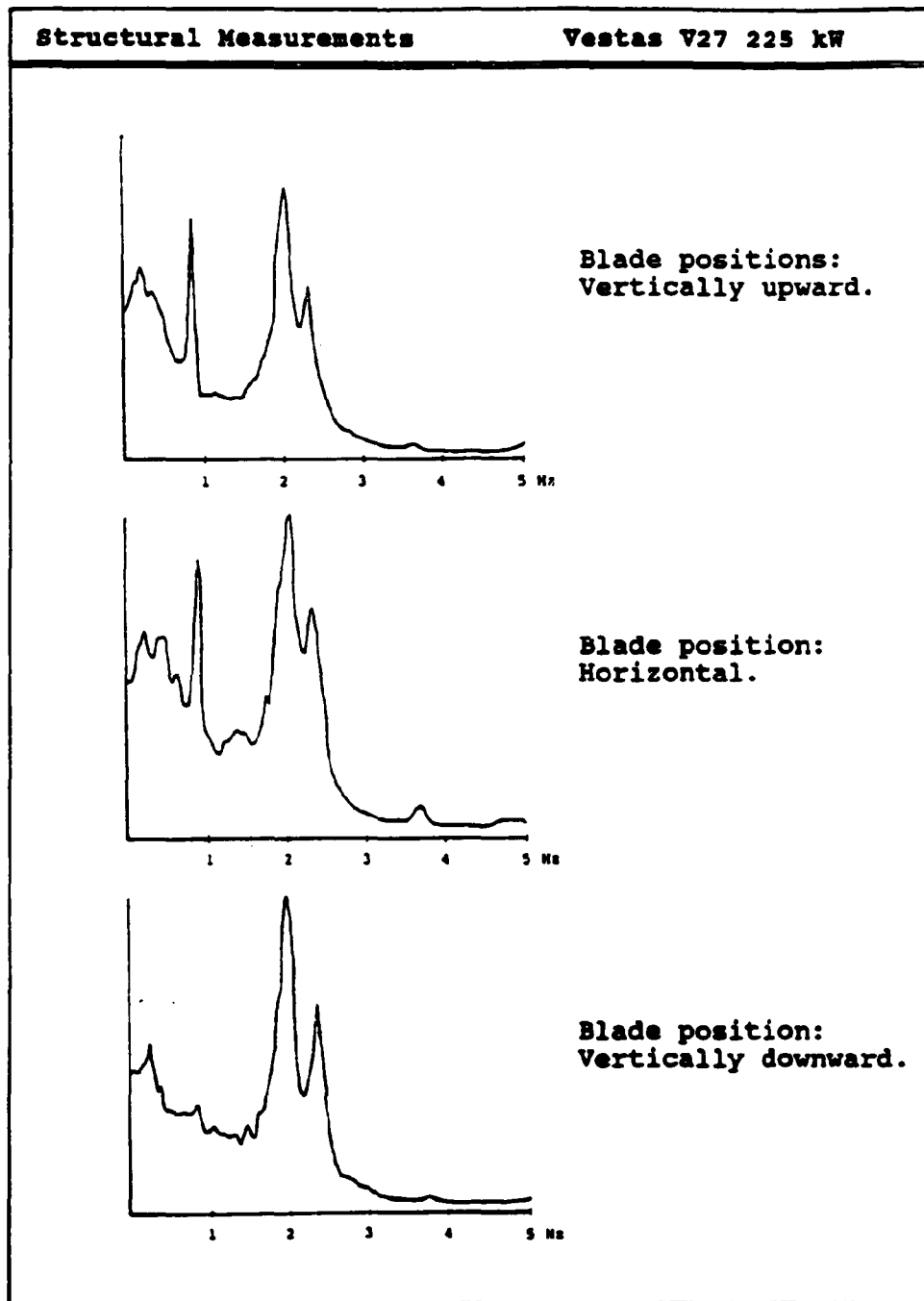


Fig. 6.1.6 *Frequency spectra of flapwise blade root bending moment at standstill in three positions.*

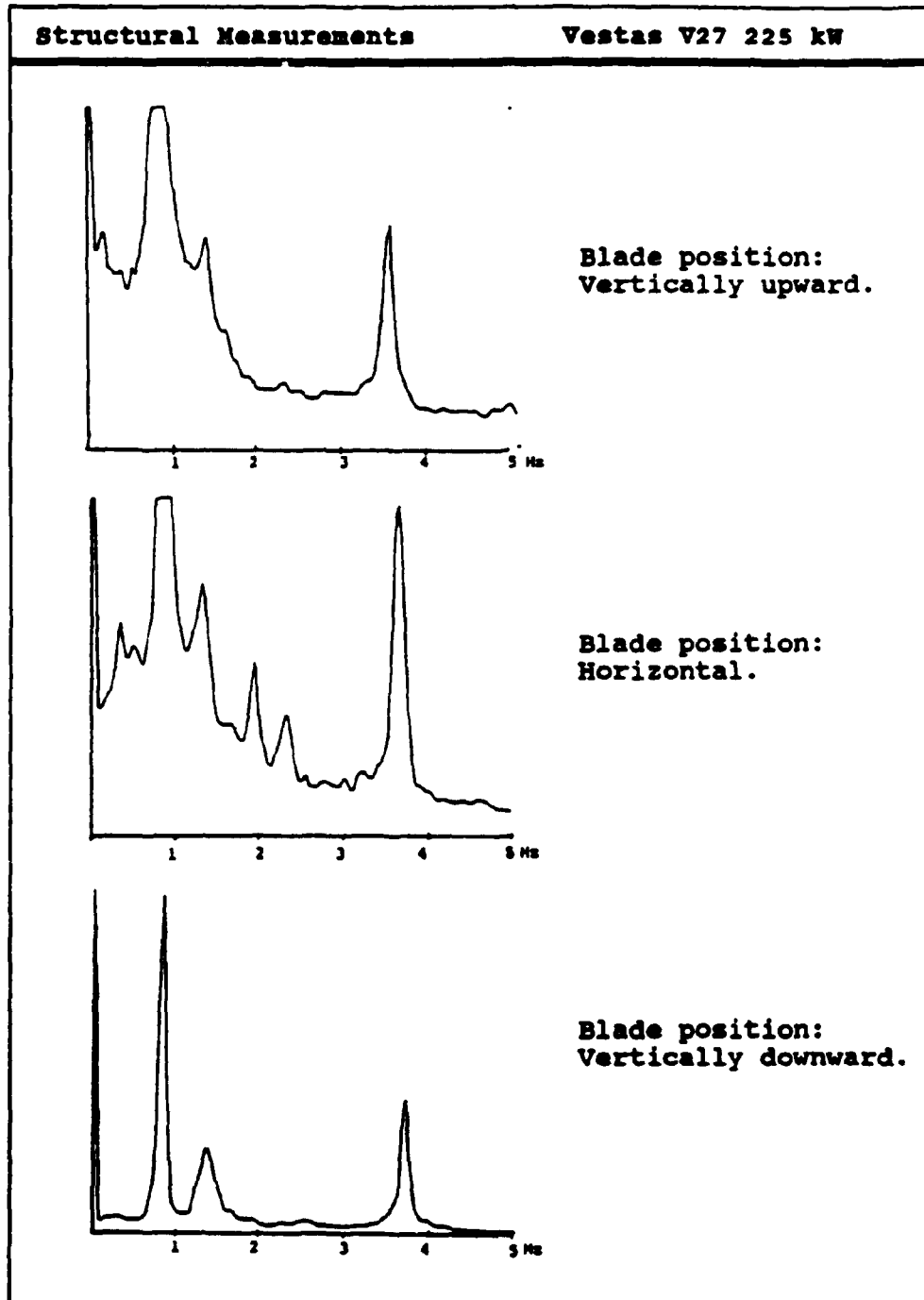


Fig. 6.1.7 Frequency spectra of edgewise blade root bending moment at standstill in three positions
(The two upper spectra are out of scale).

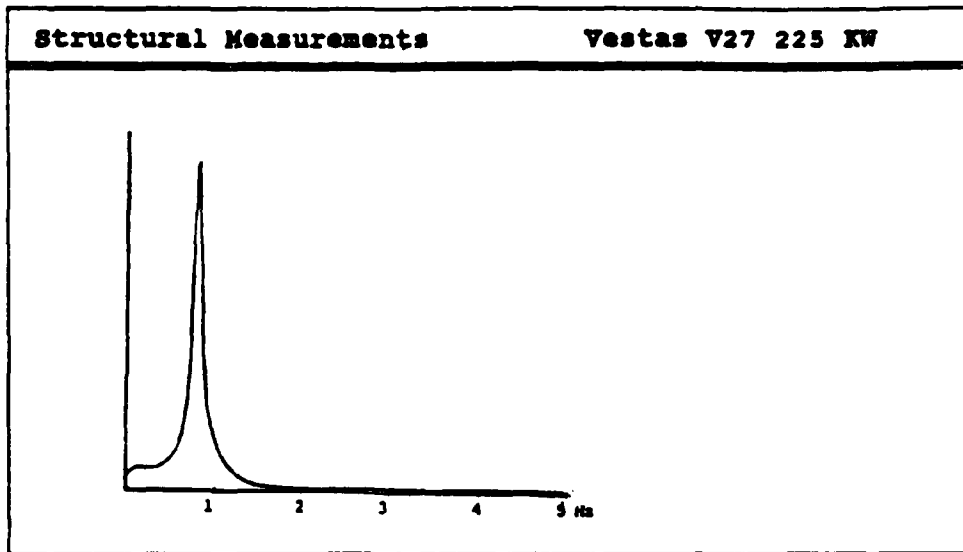


Fig. 6.1.8 Frequency spectrum of lower root bending moment at standstill.

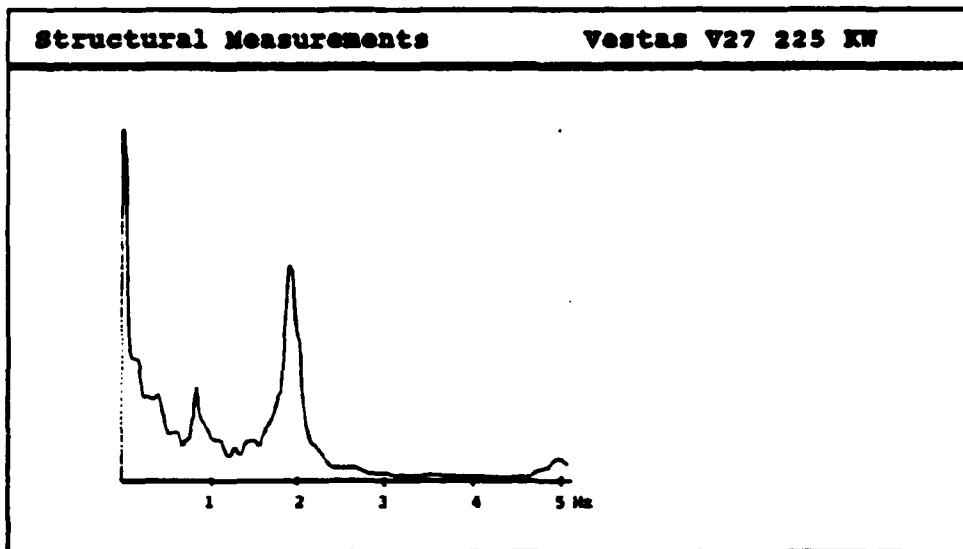


Fig. 6.1.9 Frequency spectrum of lower torsion at standstill.

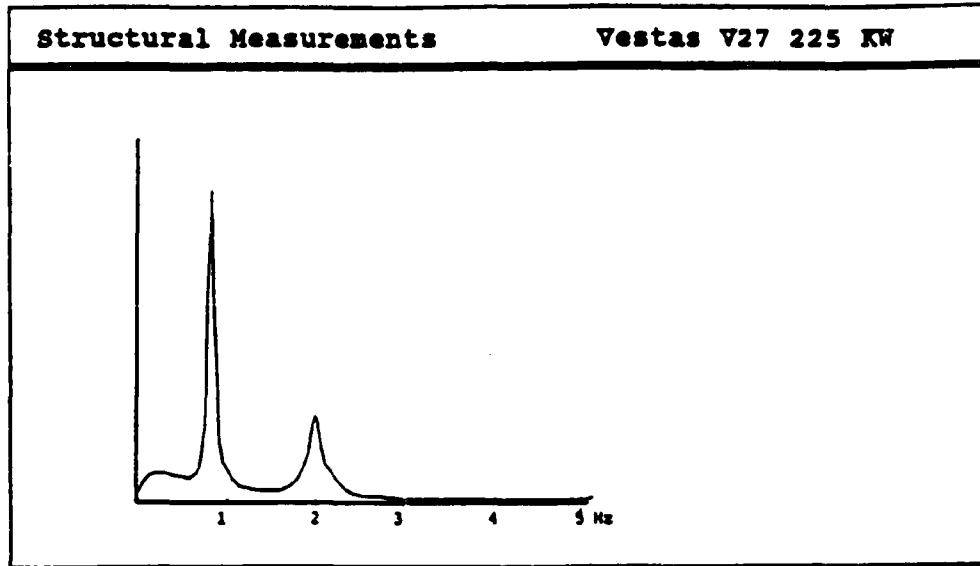


Fig. 6.1.10 Frequency spectrum of tower top bending moment at standstill.

There are also modes with higher eigenfrequencies, but due to the low energy input to these modes during normal operation, they are of minor importance.

6.2. Structural response during operation.

Unlike the situation in paragraph 6.1 the structure is now excited by cyclic loads, when the turbine is running at one of the two operational speeds, 33 rpm and 43 rpm. These cyclic loads are caused by different effects as wind shear, yaw, gravitational forces in the blades and tower influence on the flow. The dominant excitation frequencies are therefore multiples (1P, 2P, 3P ..) of the rotational speed. This means excitation frequencies of 0.72 Hz, 1.44 Hz, 2.15 Hz,... at the high rotational speed and 0.56 Hz, 1.12 Hz, 1.65 Hz,... at the low speed.

Most of the energy input to the rotor modes comes from the 1P and 3P excitation, and it is therefore important that these do not coincide with any eigenfrequencies of the structure. The frequency spectra of six different parameters for the turbine running at 43 rpm are shown in Fig. 6.2.1 to Fig. 6.2.6 (linear scale).

Probably due to some minor aerodynamic and weight unbalance all signals contains deterministic periodic parts at the rotational frequency.

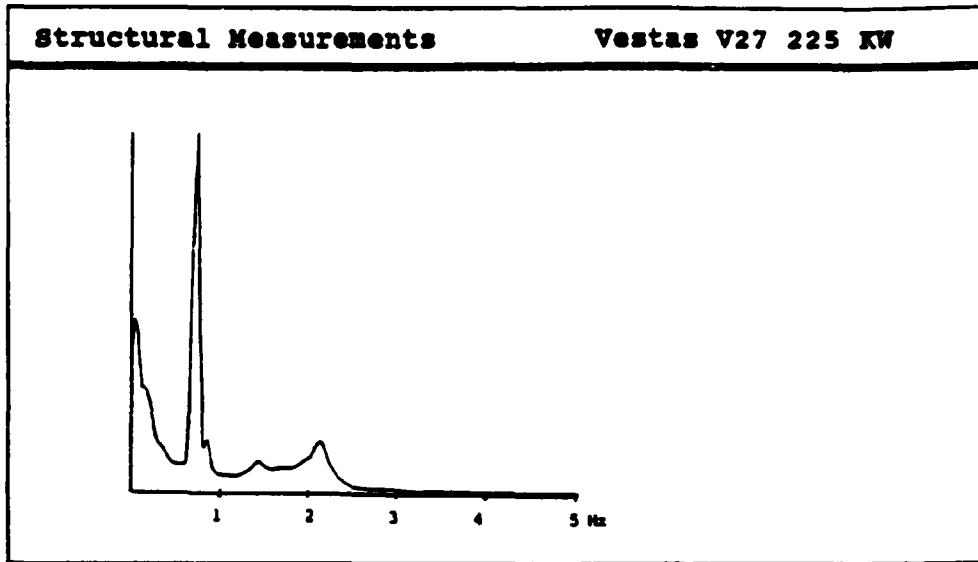


Fig 6.2.1 Frequency spectrum of the electrical power at a rotor speed of 43 rpm.

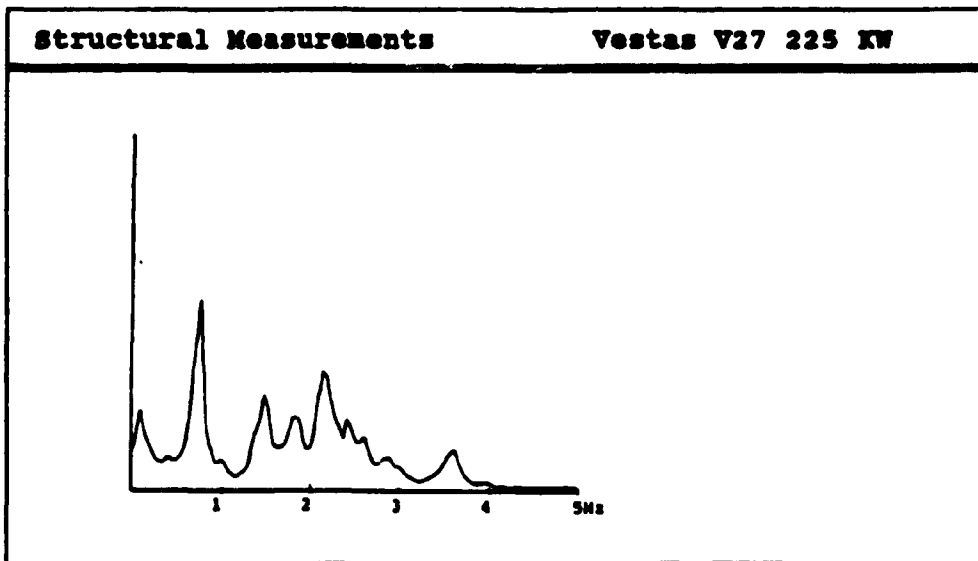


Fig 6.2.2 Frequency spectrum of the flapwise root bending moment at a rotor speed of 43 rpm.

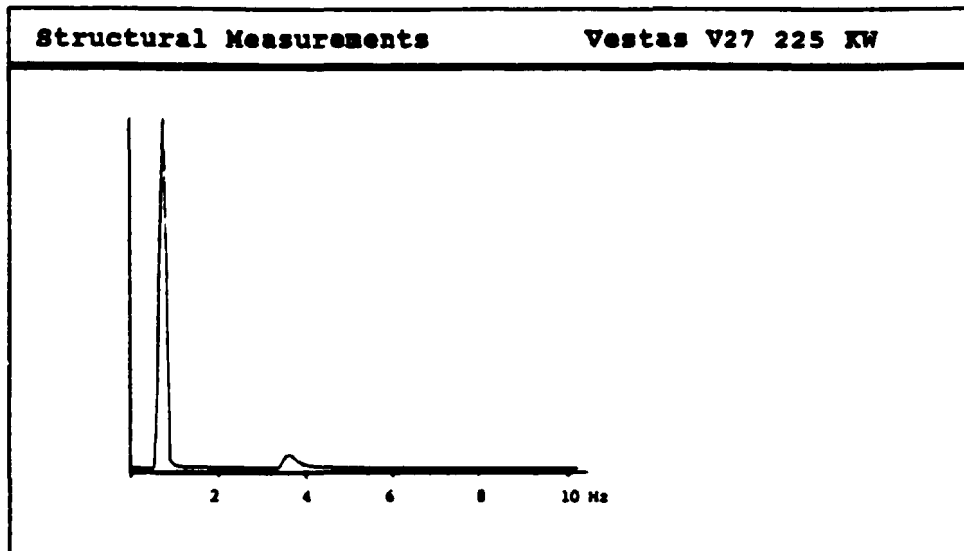


Fig 6.2.3 Frequency spectra of edgewise root bending moment at a rotor speed of 43 rpm.

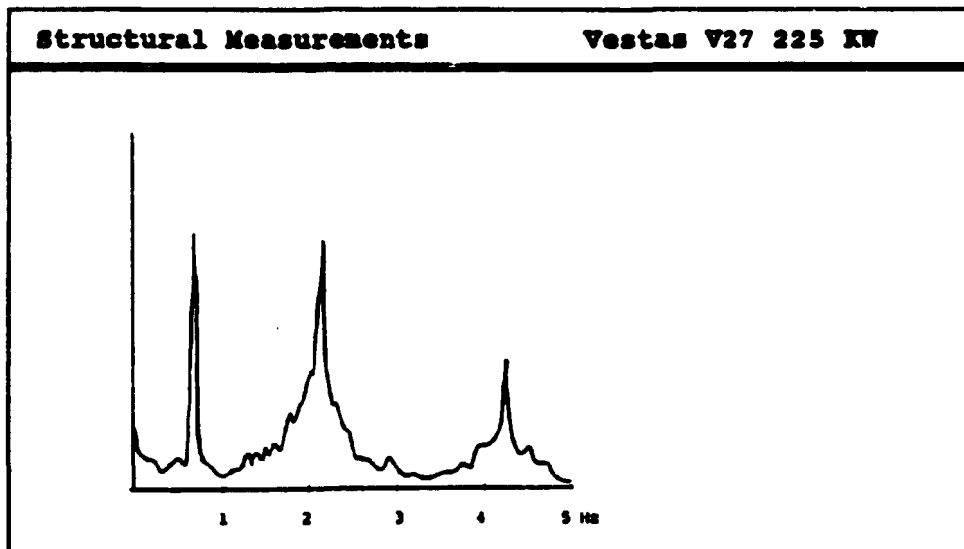


Fig 6.2.4 Frequency spectra of tower torsional moment at a rotor speed of 43 rpm.

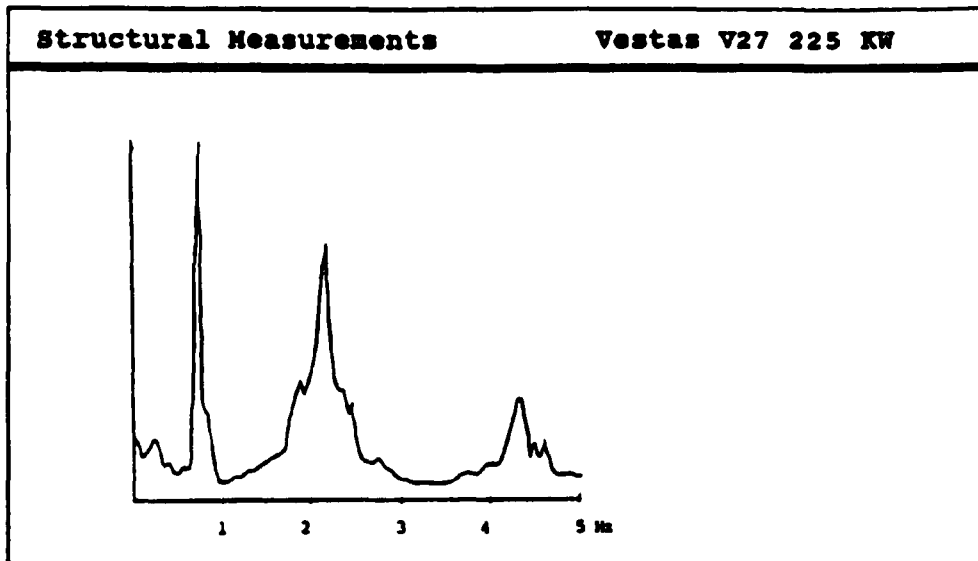


Fig 6.2.5 Frequency spectra of the tower top bending moment at a rotor speed of 43 rpm.

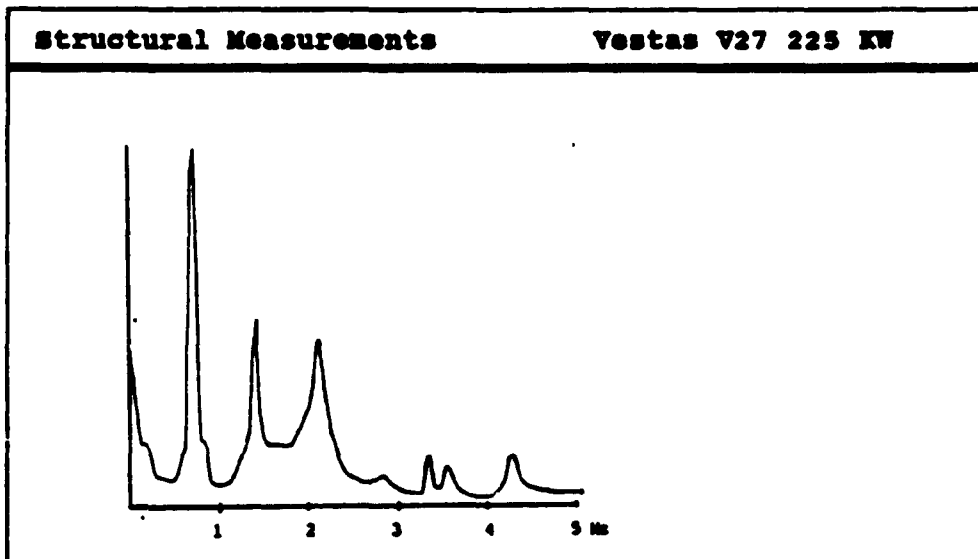


Fig 6.2.6 Frequency spectra of the rotor shaft torque at a rotor speed of 43 rpm.

The dominating frequencies in the tower spectra are seen to be the 1P, 3P and 6P. The frequency 6P is not seen in any of the other spectra.

6.3. Structural measurements summary.

The vibrational mode shapes and the eigenfrequencies measured during stand still with the pitch angle in -1 deg are:

<u>Mode</u>	<u>Dominant mode/Main coupling</u>	<u>Frequency</u>
Mode 1	1st tower bending/1st symmetric rotor, in-phase	0.84 Hz
Mode 2	1st asymmetric rotor/1st tower torsion, in-phase	1.96 Hz
Mode 3	1st asymmetric rotor/2nd tower bending, in-phase	2.00 Hz
Mode 4	1st symmetric rotor/1st tower bending, counter-phase	2.36 Hz
Mode 5	1st torsional tower/1st asymmetric rotor, counter-phase	5.04 Hz
Mode 6	1st shaft torsion/1st edgewise, in-phase	1.40 Hz
Mode 7	1st Edgewise	3.64 Hz

Mode 6 only exists when the mechanical brake is blocked, i.e. when the turbine is stopped. The rotor frequencies are slightly increased during operation.

7. MEASUREMENTS OF ELECTRICAL CHARACTERISTICS

7.1 Measurements of current at cut-in.

A cut-in sequence of the generator at 43 rpm and at a about 25% power is shown in Fig. 7.1.1. and Fig. 7.1.2. The cut-in sequence at 33 rpm is shown in Fig. 7.1.3. and Fig. 7.1.4. The electrical current is unfiltered and the signals for electrical power, rotational speed and rotor shaft torque are filtered with a 20-Hz low pass filter.

Fig. 7.1.1 shows the first part of the cut-in sequence where the thyristors are active. This period had a duration of about 2 sec. The maximum electrical current is about 500 Amp in amplitude this corresponds to 91% of the current a rated power at a grid voltage of 390 Volt and a $\cos(\phi)$ of 0.86. The rotor shaft torque during this period is almost zero and no transients are seen.

After 2 sec the signal for the electrical current is a pure sinusoidal curve. When the magnetizing of the generator has finished the pitch is regulated in order to establish normal operation.

This regulation period is shown in Fig.7.1.2. It is seen that both the rotor shaft torque and the electrical power are regulated very soft. No transient loads are seen.

Fig. 7.1.3 and Fig. 7.1.4 shows the cut-in at a rotational speed of 33 rpm. These figures shows the flapwise root bending moment instead of the rotor shaft. The cut-in strategy is exactly the same as at the high rotational speed. The shape of the electrical current is almost identical in the two cases, but the maximum electrical current is less in amplitude. The maximum current is about 180 Amp, which corresponds to 33% of the current at rated power. The flapwise root bending moment during the first period is almost zero and no transients are seen.

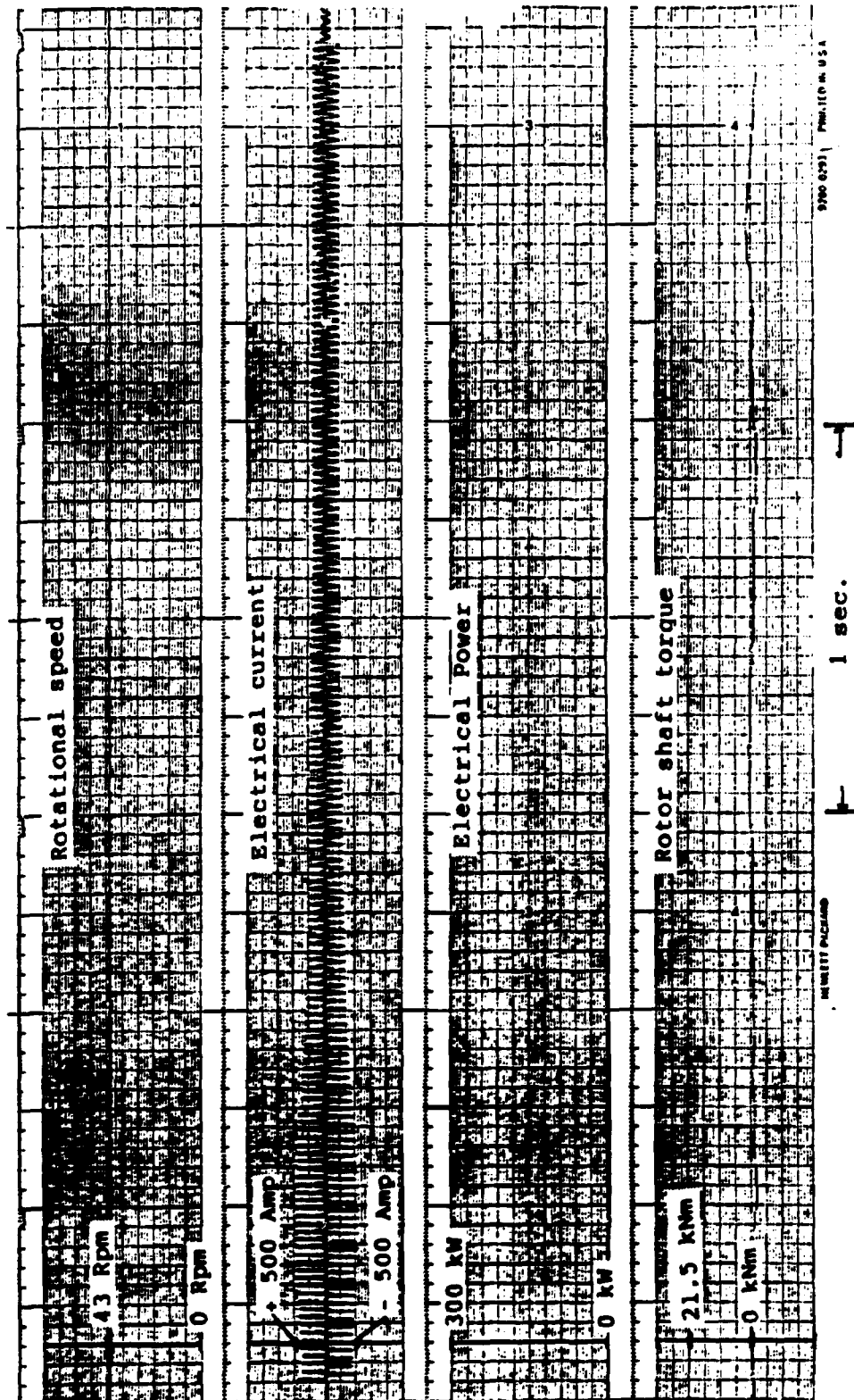


Fig. 7.1.1 Electrical current at cut-in at 43 rpm.

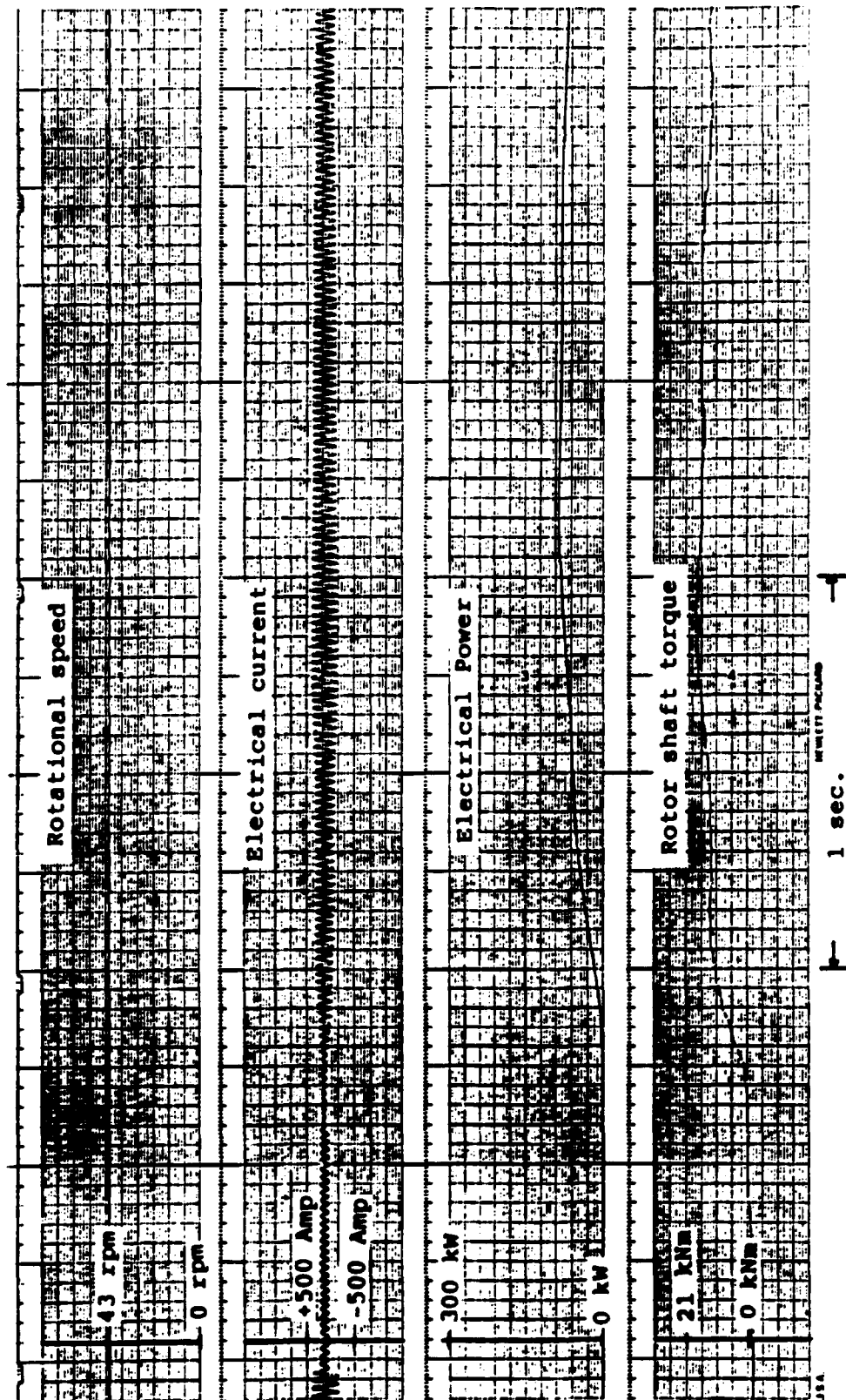


Fig. 7.1.2 Electrical current at cut-in at 43 rpm.

Fig. 7.1.3 Electrical current at cm-in at 33 rpm.

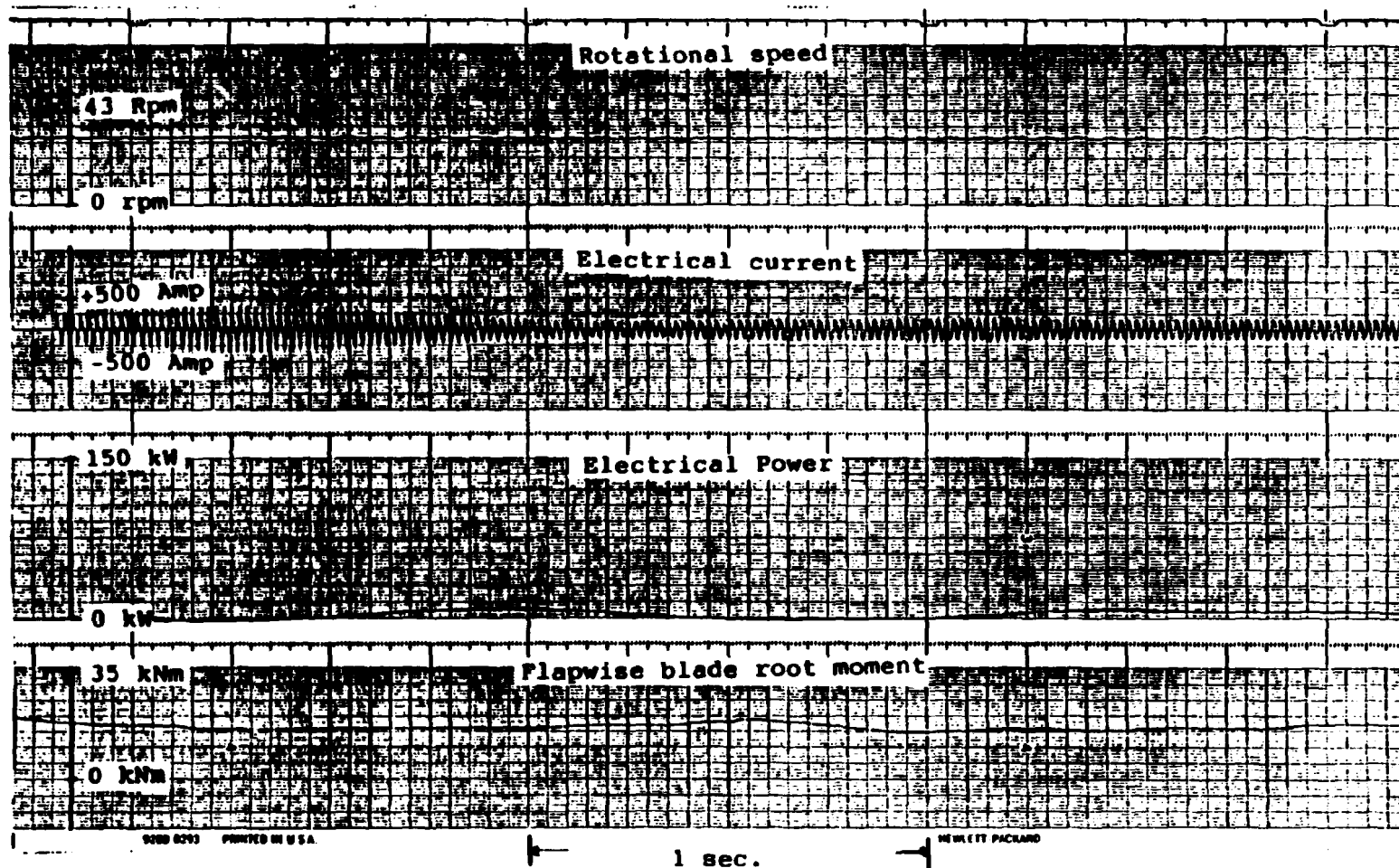
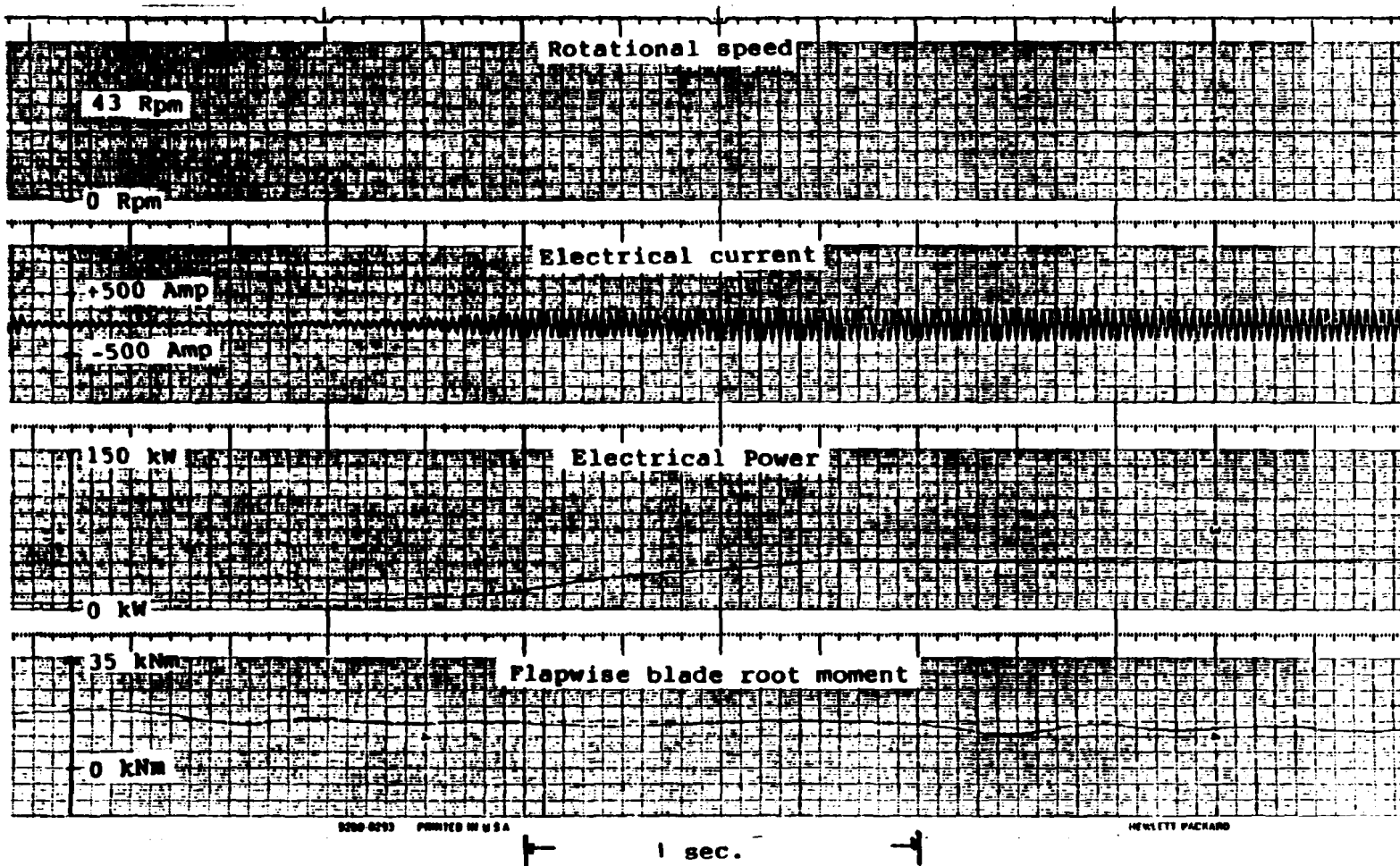


Fig. 7.1.4 Electrical current at cut-in at 33 rpm.



7.2. Electric power quality.

The power quality is described through time tracks of the electrical power, wind speed and pitch angle in Fig. 7.2.1. and Fig. 7.2.2.

Fig. 7.2.3 and Fig. 7.2.4 shows dot plots of the standard deviation of the electrical power and the wind speed respectively as function of the wind speed during 10 minutes periods.

Fig. 7.2.5 shows dot plots of the mean-, max- and min-value during 10 minute periods together with the standard deviation.

The time tracks in Fig. 7.2.1 are recorded at a wind condition where the turbine is operating with constant pitch angle and the time tracks in Fig. 7.2.2. are recorded at high wind speed where the turbine is operating with variable pitch angle.

From Fig. 7.2.1 it is seen that the correlation between wind speed and electrical power is rather good. From Fig. 7.2.3 it is seen that the standard deviation range from about 15 to 45 kW at a mean wind speed of 8 m/s. The corresponding standard deviation of the wind speed at 8 m/s range from 0.6 to 2.0 m/s. This corresponds to a turbulence range between 10 and 25 %.

At high wind conditions very steep power gradients are seen as response to wind gusts. The maximum value of the power in Fig. 7.2.2 is about 295 kW. The maximum values in Fig 7.2.4 are in the range of 300 kW too. The correlation between the wind speed and the pitch angle is as expected very good in the regulation region.

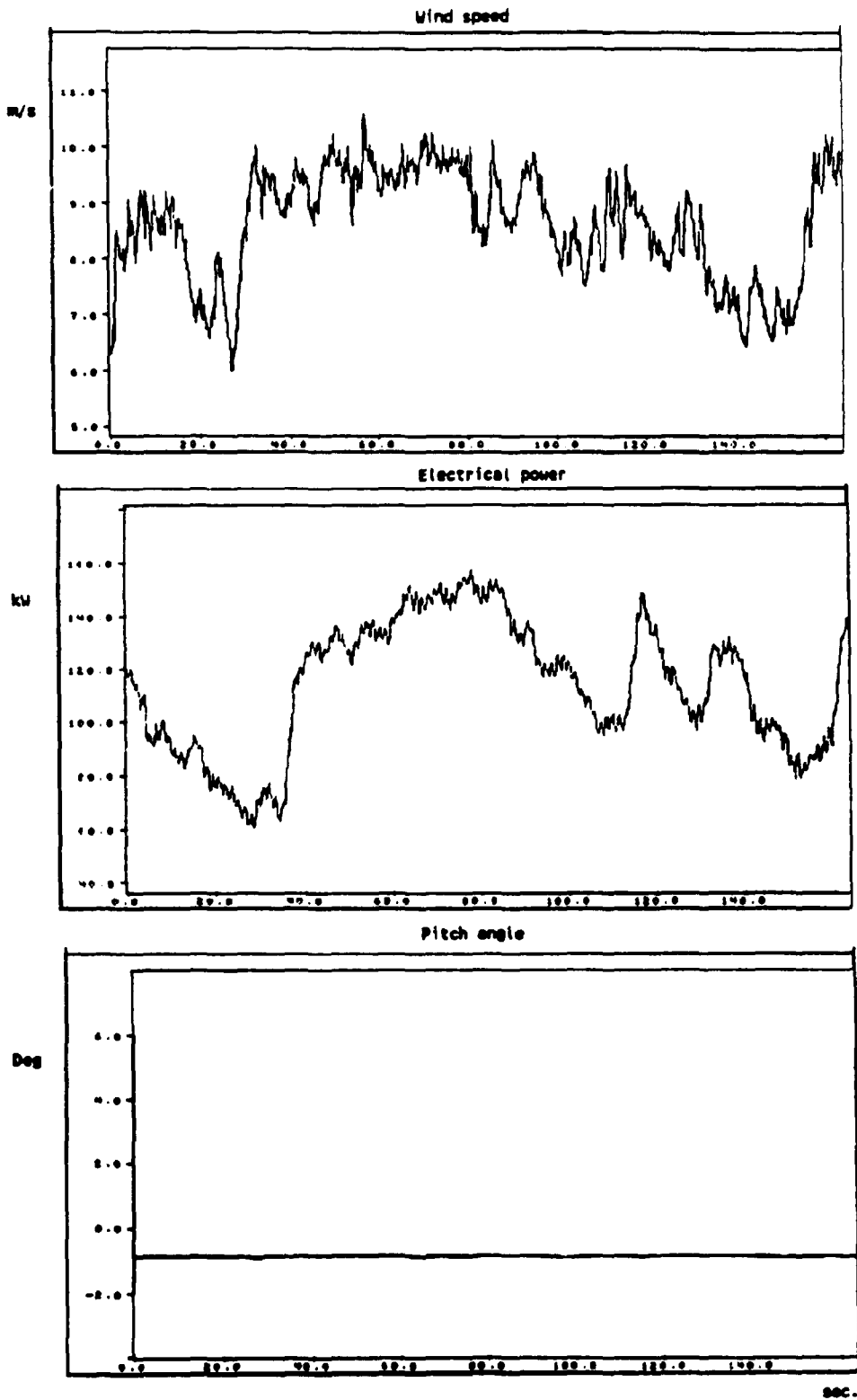


Fig.7.2.1 Power fluctuations at low wind conditions.

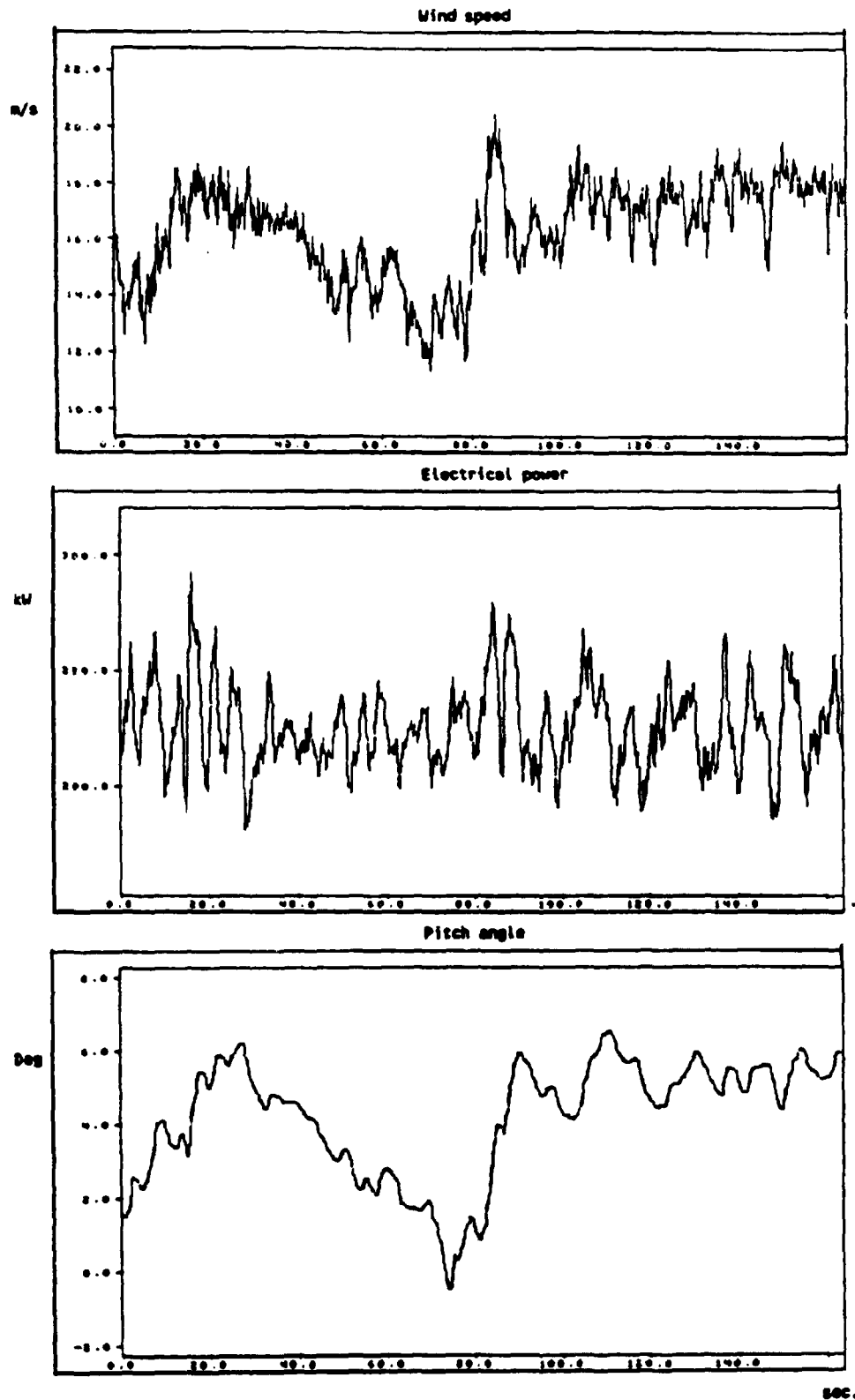


Fig.7.2.2 Power fluctuations at high wind conditions.

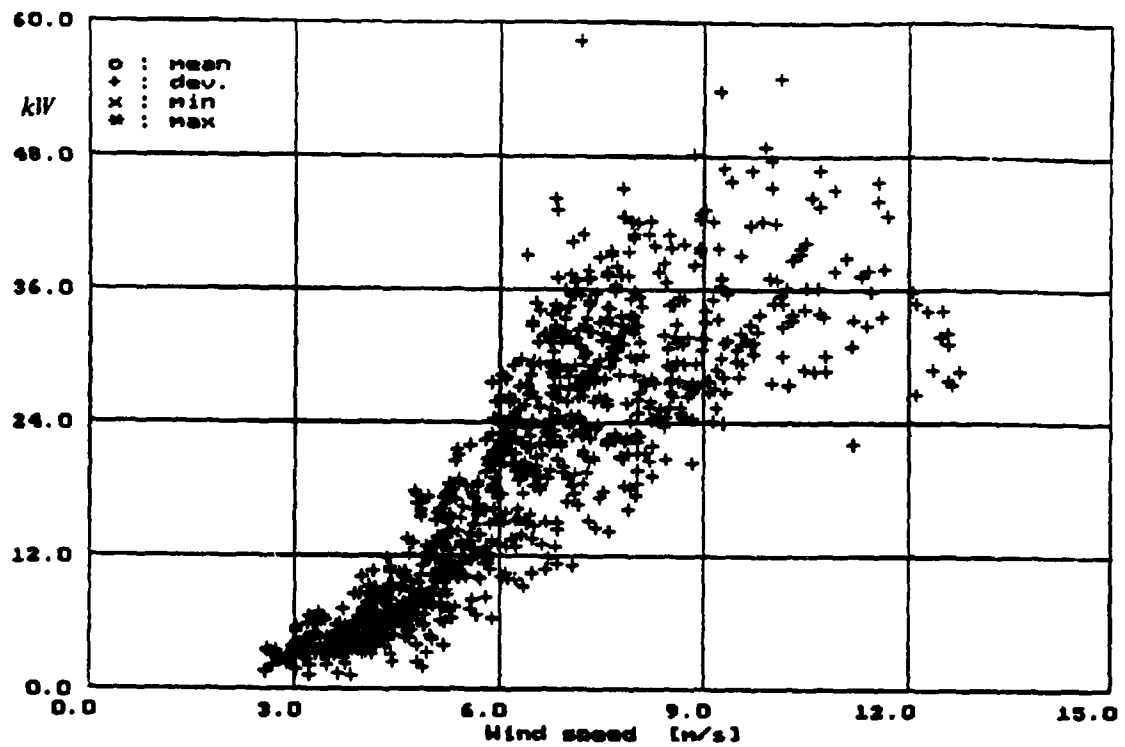


Fig.7.2.3 Standard deviation of electrical power.

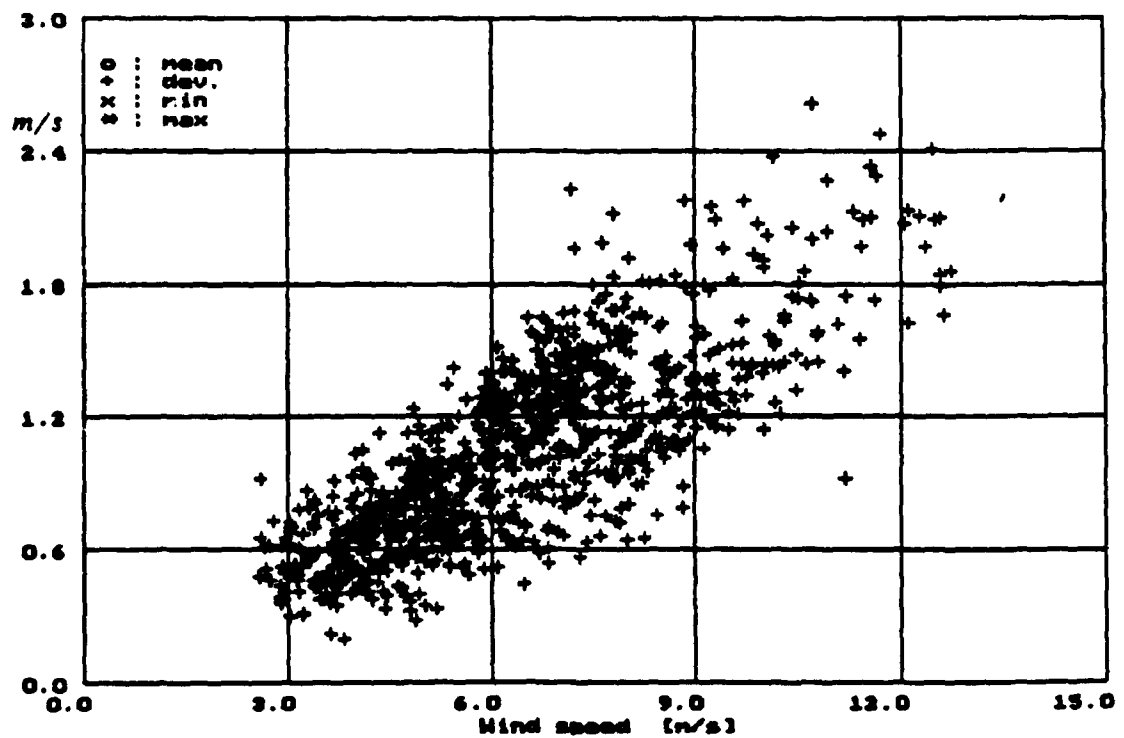


Fig.7.2.4 Standard deviation of wind speed.

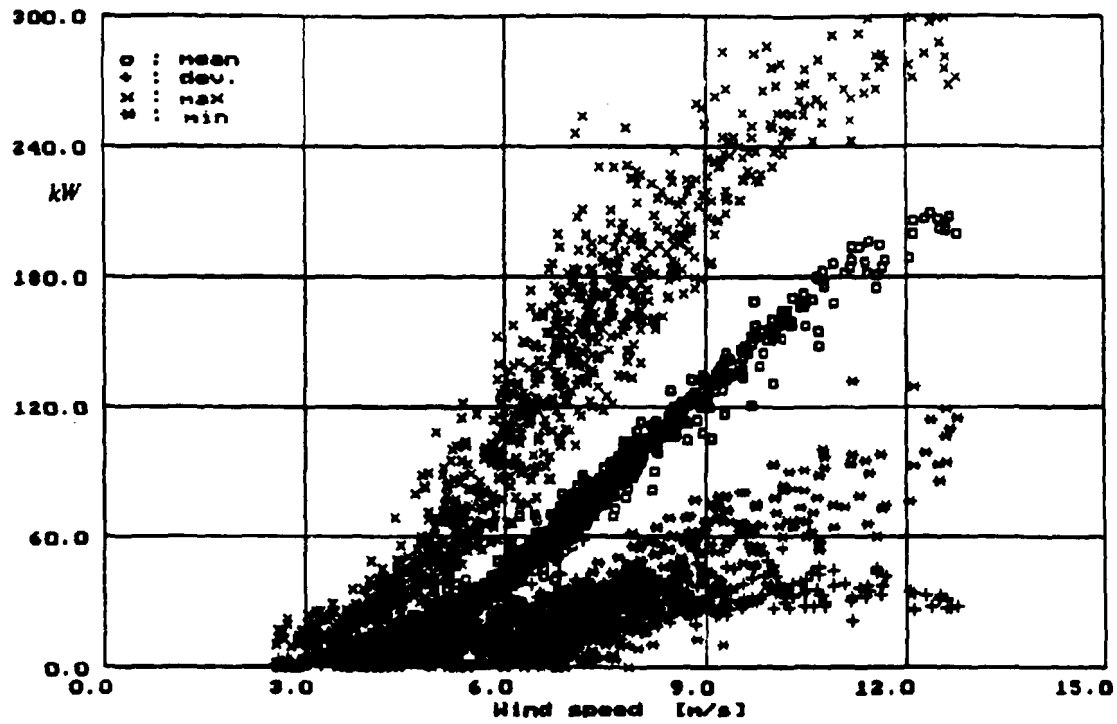


Fig.7.2.5 Mean-, max-, min-value and standard deviation of the electrical power during 10 minutes.

8. OTHER DESIGN RELATED MEASUREMENTS

8.1. Transmission efficiency.

The power train idling loss without the rotor was measured in the Test Station's workshop.

When operating as motor at low rpm the idling loss was 5.34 kW, at a gearbox temperature of 18 deg(c). As the oil temperature was increasing to a constant level of 32 deg(c) the idling loss was decreasing to 3.79 kW.

The transmission efficiency of the turbine in operation was measured as described in Chapter 3.2. The bin parameter was the electrical power and the bin width was 5 kW. Measurements were started the 6th of October-89 totalling 69 hours of measurement time. The transmission efficiency is shown when the turbine was operating fully at low or high operational speed respectively. The result is shown in Fig. 8.1.1 and in Table 8.1.2.

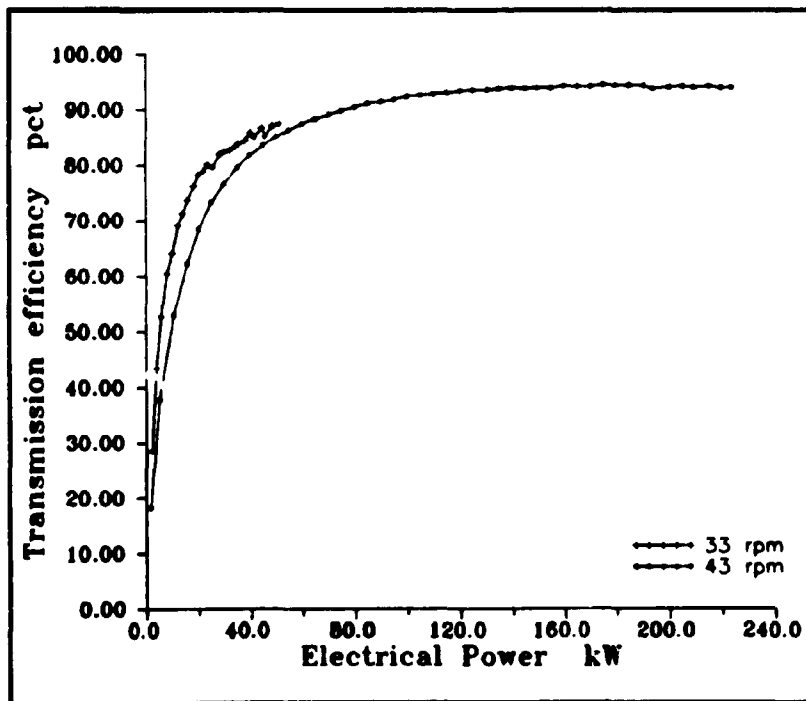


Fig. 8.1.1. Transmission efficiency.

Table 8.1.2. Tabulated data for transmission efficiency.

Measurement period: 6. oct 1989
 Measurement time: 69 hours
 Measured data curve: Transmission Efficiency
 X1: Transmission efficiency (43 rpm) (%)
 Y1: Electrical power (43 rpm) (kW)
 X2: Transmission efficiency (33 rpm) (%)
 Y2: Electrical power (33 rpm) (kW)

X1	Y1	X2	Y2
1.90	18.35	2.14	28.55
5.20	37.82	4.02	43.47
10.56	53.00	5.96	52.72
15.57	62.30	7.97	60.49
20.11	68.42	9.95	64.14
25.24	73.36	12.19	69.13
29.86	76.55	14.02	71.26
35.16	79.62	15.80	73.70
39.84	81.88	18.11	76.22
45.03	83.66	19.95	78.32
50.01	85.21	22.16	78.86
54.90	86.39	23.79	80.16
60.03	87.56	25.68	79.57
64.84	88.40	28.31	82.05
70.00	89.19	30.00	82.48
74.88	89.88	32.25	82.83
79.86	90.50	34.36	83.45
84.88	91.21	35.55	83.95
89.69	91.48	38.08	84.46
94.93	91.93	40.06	85.95
99.97	92.47	41.53	85.12
104.89	92.66	44.55	86.75
110.00	92.93	45.79	85.22
114.93	93.19	48.64	87.11
120.06	93.54	51.36	87.49
124.91	93.64		
130.43	93.70		
134.81	93.94		
139.88	94.04		
144.98	94.00		
149.56	94.10		
154.79	94.06		
159.70	94.40		
164.90	94.34		
170.24	94.31		
175.04	94.59		
179.63	94.54		
184.76	94.52		
190.62	94.48		
194.01	93.99		
200.07	94.24		
205.19	94.36		
209.30	94.19		
214.98	94.37		
219.72	94.12		
223.45	94.15		

The maximum transmission efficiency is 94.6% at about 175 kW. Below 60 kW the efficiency drops off when operating at high rpm. In the region up to about 40 kW the turbine was operating at 33 rpm. The maximum power measured when operating at 33 rpm was 51.4 kW. At this condition the transmission efficiency was 87.5%, which was the maximum transmission efficiency.

8.2. Rotor Performance.

The power delivered from the rotor shaft to the nacelle is a measure of the ability of the wind turbine blades to extract energy from the wind.

The rotor shaft power is calculated from the measurements of the power curve and the transmission efficiency. Interpolation is used for the transmission efficiency. The mechanical power curves and the rotor efficiencies at low and high rpm are shown in Fig. 8.2.1 and Fig. 8.2.2.

The maximum efficiency at low rpm is calculated to 0.63 at 4 m/s. Even a small offset error in the rotor torque measurement can cause a relatively large error on the transmission efficiency, which maybe explains the extremely high value of the rotor performance. At high rotational speed the maximum efficiency is calculated to 0.56 at 7.0 m/s. The maximum mean-value of the mechanical power output is 250 kW at a wind speed of 18.2 m/s.

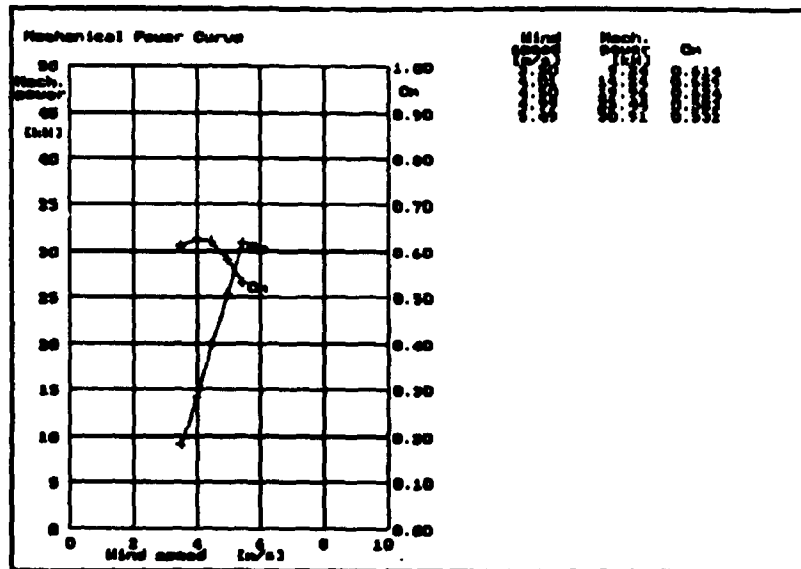


Fig. 8.2.1. Mechanical power curve at low rpm.

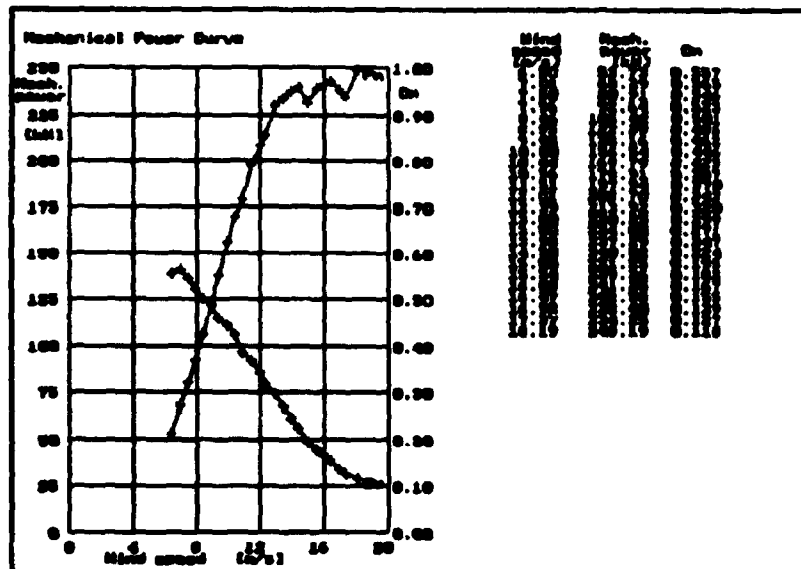


Fig. 8.2.1. Mechanical power curve at high rpm.

8.3. Yaw error measurements

Yaw error is the difference between the average wind direction and the average direction of the rotor axis.

Yaw error causes cyclic aerodynamic blade load, and can contribute significantly to the fatigue load, especially of the blade. Therefore yaw measurements during normal operation are applicable for prediction of the fatigue life as well for the blade as well for other component exposed for fatigue loads.

The sampled data are averaged over 30 seconds and the standard deviation is calculated. Inside each bin the min-max value and of the yaw error are found and the standard deviation is calculated. The result is shown in Fig. 8.3.1 and tabulated in Table 8.3.2.

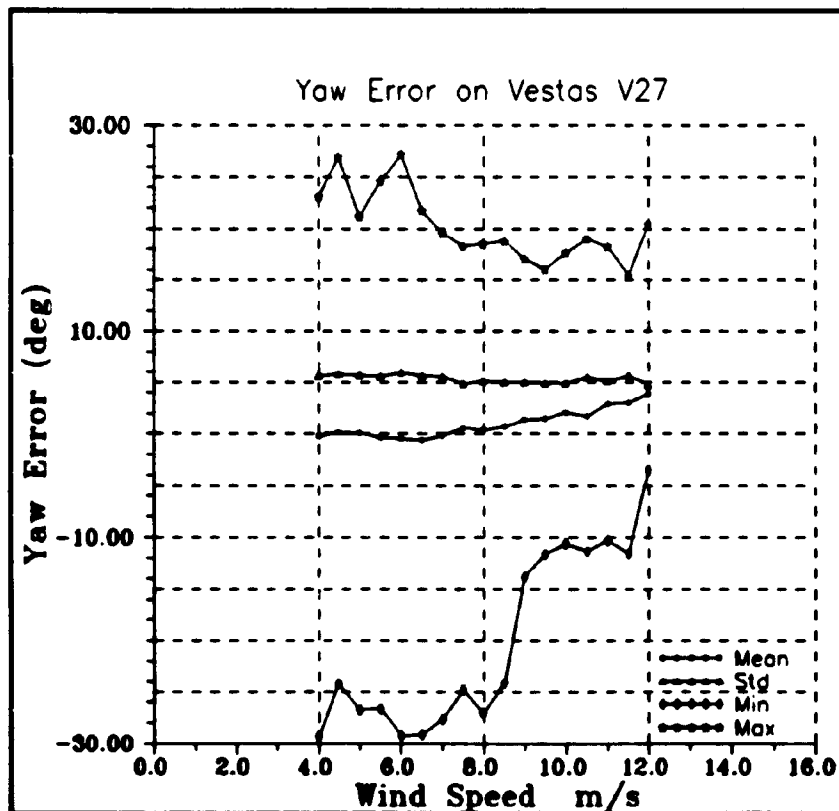


Fig. 8.3.1. Yaw errors as function of wind speed.

The result is a rather constant value of the yaw error close to zero degree at wind speeds up to 8 m/s. At higher wind speeds the yaw error rises slightly up to 4 deg at 12 m/s with a tendency to increase at higher wind speeds. The result also shows that the standard deviation of the yaw error with a reasonable approximation is independent of the wind speed. This indicates that the control system performs the yawing satisfactorily during the measured operational range.

The probability distribution of the yaw error is measured for 2 different wind speed ranges 5-7 m/s and 9-11 m/s respectively. Fig. 8.3.3 and Fig. 8.3.4 shows the distribution. It appears there is a reasonable evidence for a normal distribution of the yaw-error.

Table 8.3.2. Data for yaw error as function of wind speed.

Measurement period: 14-oct-89

Measurement time: 135 hours

Measured data curve: Yaw error

X: Wind speed (m/s)

Y1: Mean-value of yaw error (deg)

Y2: STD-value of yaw error (deg)

Y3: Min-value of yaw error (deg)

Y4: Max-value of yaw error (deg)

X	Y1	Y2	Y3	Y4
4.00	-0.26	5.64	-29.30	23.10
4.49	0.10	5.81	-24.23	26.95
5.00	0.05	5.72	-26.78	21.15
5.50	-0.37	5.60	-26.66	24.56
6.01	-0.47	5.99	-29.29	27.21
6.51	-0.64	5.63	-29.14	21.74
7.00	-0.20	5.58	-27.69	19.54
7.50	0.55	4.85	-24.84	18.28
7.98	0.37	5.14	-27.08	18.51
8.49	0.69	5.04	-24.12	18.77
8.99	1.37	5.02	-13.84	17.06
9.49	1.50	4.91	-11.66	16.05
9.99	2.09	4.90	-10.61	17.62
10.50	1.70	5.50	-11.36	19.00
11.00	2.92	5.11	-10.30	18.23
11.51	3.03	5.66	-11.59	15.40

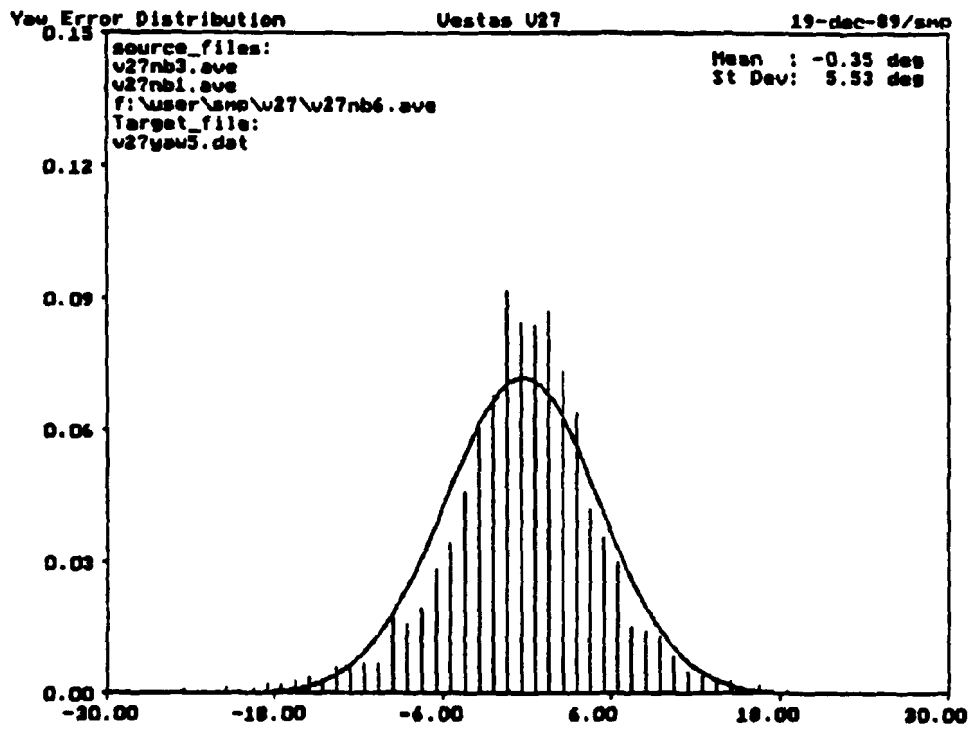


Fig. 8.3.3. Probability distribution of yaw error at 5 to 7 m/s.

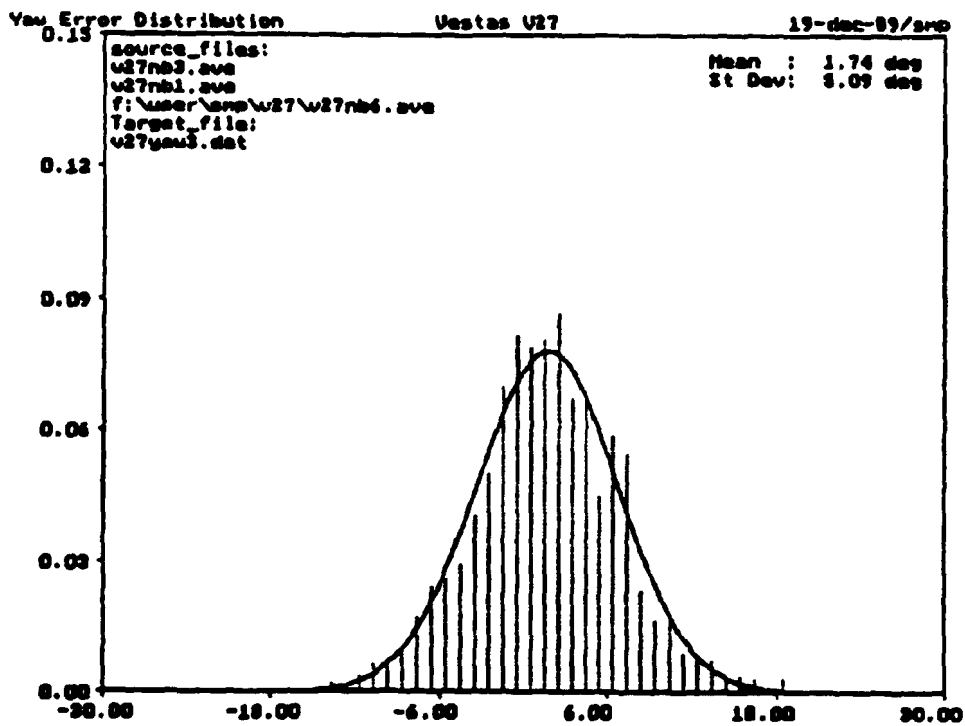


Fig 8.3.4. Probability distribution of yaw error at 9 to 11 m/s.

8.4 Flapwise root bending moment

The flapwise blade bending moment is shown in Fig. 8.4.1. The measurements are block averaged to 10 minutes. The mean-, max- and min-values of the block averages are plotted against the wind speed.

Important to note is that the flapwise bending moment is measured on the pitching blade and corrected to rotor centrum. To get the bending moment in and out of the rotor plane the flapwise bending moment should be corrected for the pitching angle. The data presented in Fig. 8.4.1 are not corrected for the centrifugal de-loading either. By centrifugal de-loading is meant that the total flapwise blade bending moments during operation is lowered due to an opposite bending moment from the centrifugal forces on the deflected blade see Ref 6.

The de-loading can be calculated when the stiffness and mass distribution of the blade is known. For the actual blade the de-loading in the root section is in the range of 5 %.

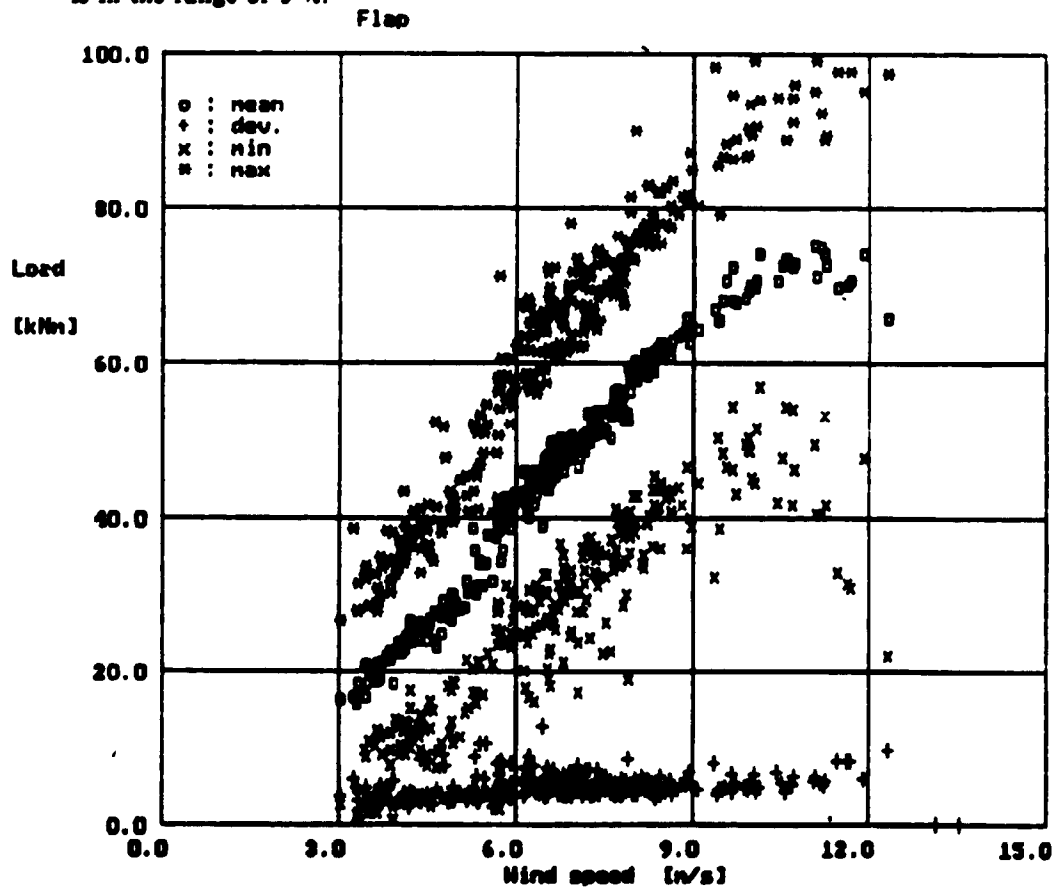


Fig 8.4.1. Flapwise root bending moment corrected to rotor centrum.

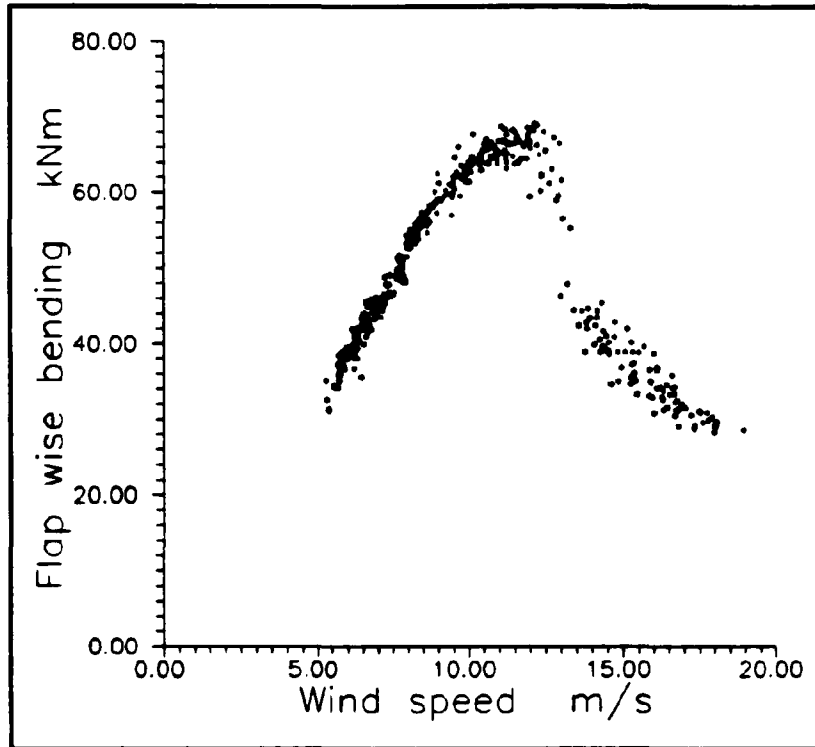


Fig 8.4.2 Flapwise bending at a radius of 0.9 m

Fig. 8.4.2 shows the mean value of the flap wise bending moment at radius of 0.9 m. Compared to Fig. 8.4.1 the curve is also extended with data at high wind speeds from 12 to 18 m/s based on 30 sec average.

8.5 Axial rotor thrust

The axial rotor thrust is shown in Fig. 8.5.1. The measurements are block averaged to 10 minutes. The mean-, max- and min-value of the block averages are plotted against the wind speed.

The thrust is deduced from the tower root bending moment, assuming that the force is acting in the rotor center. There is not made compensation for the drag on the tubular tower.

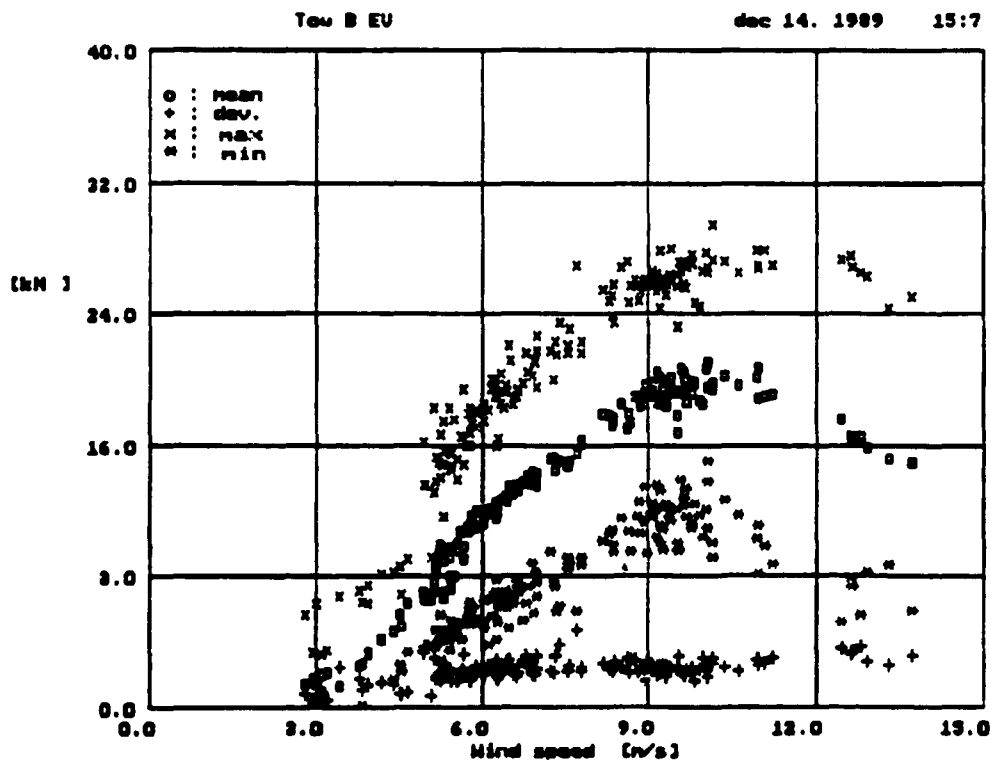


Fig 8.5.1. Axial rotor thrust.

SUMMARY

The test comprised measurements and analysis concerning the safety system, performance, structural dynamics, electric characteristics, yaw statistics, flapwise blade bending moments and rotor thrust.

The mechanical brake were tested at a electrical power of approximately 90 kW and 220 kW, by disconnecting the main switch or using the "Emergency" or "Pause" button. In all cases the rotor was stopped after a safe brake sequence. The average brake torque was 56 kNm and the maximum torque was 64 kNm. The average brake torque corresponds to 1.21 times the rotor torque at rated power. A drive train eigenfrequency of 5.2 Hz was seen during that period. A overspeed of 7% was measured.

A normal shut down of the turbine were performed at a power of 80 kW and at a power of 210. In these situations the pitch regulation were activated and the electrical power and torque were decreased simultaneously in a time short time span. No significant loads in the drive train system were measured.

The efficiency of the air brakes was measured for a free running rotor with the blade turned approximately 88 degrees. The rotor was in upwind position during the test. In these conditions the rotational speed was kept below 2 rpm up to a wind speed of 25 m/s.

The performance measurements show a maximum overall efficiency of 49.5% at 7.0 m/s and a maximum power of 236 kW at 18 m/s. The pitch regulation limits the average power output to about 225 kW. The calculated energy production shows 304, 471 and 643 MWh for Rayleigh distributed wind speeds with annual mean wind speeds of 5, 6 and 7 m/s. The corresponding annual energy productions per square meter are 531, 822 and 1122 kWh/m².

The maximum transmission efficiency is 94.6% at about 175 kW. Below 60 kW the efficiency drops off when operation at the main generator. The maximum transmission efficiency when operation at the low rpm was 87.5%. The maximum rotor efficiency at high rpm was 56.5% at 7 m/s, which must be considered to be quite high. The rotor had no starting problems due to an efficient and reliable start up mechanism.

The current during cut-in was measured at high and low rpm. In both cases the maximum current is less than the current at rated power. The power and rotor torque was regulated very soft and no transients were seen.

Power fluctuation were measured during low and high wind conditions. Typical standard deviations during 10 minutes of 15-45 kW were seen at 8 m/s.

The measurements of structural dynamics revealed 7 essential eigenfrequencies, but no serious excitation of any of them. The frequencies are: first tower bending/1st symmetric rotor 0.84 Hz, 1st asymmetric rotor/1st tower torsional 1.96 Hz, 1st asymmetric rotor/second tower bending 2.00 Hz, 1st symmetric rotor/first tower bending counter-phase 2.36 Hz, 1st torsional tower/1st asymmetric rotor, counter-phase 5.04 and finally the 1st edgewise 3.64 Hz.

The yaw error measurements shows that the control system perform the yawing satisfactory. The yaw error follow a Gauss distribution with a mean value close to zero degree. The standard deviation is about 5.5 deg. at all wind speeds.

The flap wise root bending moment and axial rotor thrust were measured as function of wind speed.

REFERENCES

1. **"GUIDANCE FOR TEST OF WIND TURBINES"** (Danish). *Troels Friis Pedersen, The Test Station for Wind Turbines, Risø National Laboratory, Denmark. September 1985.*
2. **"ECN-217 JULY, 1989 RECOMMENDATIONS FOR AN EUROPEAN WIND TURBINE STANDARD ON PERFORMANCE DETERMINATION"**. *A. Curvers, ECN, Petten, The Netherlands; T.F. Pedersen, The Test Station for Wind Turbines, Risø National Laboratory, Denmark. July 1989.*
3. **INSTRUKTIONSBOG VESTAS VINDMØLLE V27-200.** *Vestas.*
4. **"STANDARD MEASUREMENTS ON WIND TURBINES AT THE TEST STATION FOR WIND TURBINES AT RISØ, DENMARK"**. *Troels Friis Pedersen, The Test Station for Wind Turbines, Risø National Laboratory, Denmark. 1983.*
5. **"WIND ATLAS FOR DENMARK"**. *Erik Lundtang Petersen, Ib Troen, Steen Frandsen, Department of Meteorology and Wind Energy, Risø National Laboratory, Denmark. 1980.*
6. **"INVESTIGATIONS OF AERODYNAMICS, STRUCTURAL DYNAMICS AND FATIGUE ON DANWIN 23 180 KW"**. *Flemming Rasmussen, et al., The Test Station for Wind Turbines, Risø National Laboratory, Denmark. 1988.*

Title and author(s) WIND TURBINE TEST VESTAS V27-225 kW <i>Søren Markkilde Petersen</i>	Date October 1990
	Department or group The Test Station for Wind Turbines
	Groups own registration number(s)
	Project/contract no.
Pages 66 Tables 5 Illustrations 43 References 6	ISBN 87-550-1684-7
Abstract (Max. 2000 char.) <p>Abstract. The report describes fundamental measurements performed on a Vestas-V27-225 kW pitch regulated wind turbine. The measurements carried out and reported here comprises the power output, system efficiency, energy production, transmission efficiency, rotor power, rotor efficiency, air-brakes efficiency, structural dynamics, loads at cut-in and braking, yaw error statistics, flapwise root bending moment and rotor thrust.</p>	
Descriptors - EDB BRAKES; DYNAMIC LOADS; HORIZONTAL AXIS TURBINES; MECHANICAL TESTS; PERFORMANCE TESTING; POWER GENERATION; ROTORS	
<small>Available on request from Riso Library, Riso National Laboratory, (Riso 5500000, Postbokscenter Riso).</small>	